Distributed coordination control for multi-robot networks using Lyapunov-like barrier functions

Dimitra Panagou, Dušan M. Stipanović and Petros G. Voulgaris

Abstract

This paper addresses the problem of multi-agent coordination and control under multiple objectives, and presents a set-theoretic formulation amenable to Lyapunov-based analysis and control design. A novel class of Lyapunov-like barrier functions is introduced and used to encode multiple, non-trivial control objectives, such as collision avoidance, proximity maintenance and convergence to desired destinations. The construction is based on recentered barrier functions and on maximum approximation functions. Thus, a single Lyapunov-like function is used to encode the constrained set of each agent, yielding simple, gradient-based control solutions. The derived control strategies are distributed, i.e., based on information locally available to each agent, which is dictated by sensing and communication limitations. Furthermore, the proposed coordination protocol dictates semi-cooperative conflict resolution among agents, which can be also thought as prioritization, as well as conflict resolution with respect to an agent (the leader) which is not actively participating in collision avoidance, except when necessary. The considered scenario is pertinent to surveillance tasks and involves nonholonomic vehicles. The efficacy of the approach is demonstrated through simulation results.

I. Introduction

Multi-agent systems have seen increased interest during the past decade, in part due to their relevance to many research domains and real world applications. Depending on the global and local/individual objectives, various distributed coordination and control problems have been introduced, namely consensus (also seen as agreement/synchronization/rendezvous), formation, distributed optimization and distributed estimation; for a recent survey on the related topics the reader is referred to [1].

When it comes to multi-vehicle systems in particular, a common ground may be that multiple agents need to work together in a collaborative fashion in order to achieve one or multiple common goals. Coordination and control in such cases is naturally dictated by the available patterns on sensing and information sharing, as well as by physical/environmental constraints and inherent limitations (e.g., motion constraints, obstacles, unmodeled

This work has been supported by Qatar National Research Fund under NPRP Grant 4-536-2-199 and AFOSR grant FA95501210193.

Dimitra Panagou is with the Department of Aerospace Engineering, University of Michigan, Ann Arbor; dpanagou@umich.edu.

Dušan M. Stipanović is with the Coordinated Science Laboratory and the Industrial and Enterprise Systems Engineering Department, University of Illinois at Urbana-Champaign; dusan@illinois.edu.

Petros G. Voulgaris is with the Coordinated Science Laboratory and the Aerospace Engineering Department, University of Illinois at Urbana-Champaign; voulgari@illinois.edu.

disturbances, input saturations etc). Therefore, the problem of motion planning, coordination and control has been and still remains an active topic of research within both the robotics and control communities. While it is out of the scope of this paper to provide an overview of the existing methodologies on these topics, the interested reader is referred to [1], [2] and the references therein for more information.

The main concerns when coordinating the motions of multi-vehicle or multi-robot (the terms are used interchangeably) teams include inter-agent collision avoidance, convergence to spatial destinations/regions or tracking of reference signals/trajectories, maintenance of information exchange among agents and avoidance of physical obstacles. Such objectives are encountered in flocking [3]–[8], and in consensus, rendezvous and/or formation control [9]–[14]. Collision avoidance is an unnegotiable requirement in such problems, and is often addressed with potential function methods and Lyapunov-based analysis. For a recent survey on potential function methods in formation control and similar problems see [15]. It is worth mentioning that these contributions do not consider all the aforementioned control objectives. In fact, the algorithmic planning and control design in such cases is, to the best of our knowledge, a very challenging, often intractable problem, and still remains an open issue in many respects.

Recently there has been significant interest in the deployment of robotic networks (or teams) for exploration, surveillance and patrolling of inaccessible, dangerous or even hostile (indoor and outdoor) environments, such as oil drilling platforms, nuclear reactors etc, see [16]–[22] and the references therein. Solutions to the relevant problems range from combinatorial motion planning to optimization-based and Lyapunov-based methods.

A. Overview

This paper is motivated in part by surveillance applications which bring in the need for the development of multi-robot coordination and control algorithms under multiple objectives. We consider a network of mobile agents which are assigned with the task to converge and remain close to predefined goal destinations, while avoiding collisions and while maintaining connectivity, realized as preserving upper bounded distances with respect to (w.r.t.) one agent called the leader of the network. The leader is not actively trying to avoid the remaining agents (followers), and is only responsible for communicating goal destinations to them. Note that the "one leader - multiple followers" terminology adopted here does not follow the usual sense in the related literature; the agents are not assigned with the task to keep fixed distances w.r.t. a physical or virtual leader, or move in a rigid geometric formation.

We propose a motion coordination approach relying on a set-theoretic formulation [23] which is amenable to Lyapunov-like analysis and distributed control design. More specifically:

1) We introduce a class of Lyapunov-like barrier functions in order to encode multiple, non-trivial control objectives, such as collision avoidance, connectivity (interpreted as proximity) maintenance, and convergence to desired destinations. The construction is based on the concept of recentered barrier functions [24] and on the approximation functions introduced in the authors' earlier work [25]. Therefore, a single Lyapunov-like function is used to encode the constrained set of each agent, yielding simple, gradient-based control solutions. In this respect, one of the merits of the proposed Lyapunov-like barrier functions is the flexibility they offer

regarding to the composition of multiple control objectives.

2) We develop distributed coordination and control strategies for each agent, which are characterized by specific levels of decentralization in terms of information sharing. The considered decentralization levels are dictated by the type of information required for an agent to accomplish the desired objectives.

B. Contributions and Organization

The contributions of the current paper lie in:

1) The introduction of the novel class of Lyapunov-like barrier functions, which offer the flexibility to compose multiple control objectives for the multi-agent system into a single one for each agent, and thus provide a starting point for the control design and analysis.
2) The adopted set-theoretic formulation for the control design and analysis. More specifically, Nagumo's Theorem [23] provides the necessary and sufficient conditions for ensuring system safety (in terms of avoiding collisions and maintaining connectivity), and therefore alleviates the standard control design practice on forcing a common (or multiple) Lyapunov function(s) to always decrease along the system trajectories, as it is often done in the related literature.
3) The consideration of nonuniform agents in terms of assigned objectives and sensing/ communication capabilities. In particular, we consider a single heterogeneous agent (the leader) who is not involved in ensuring collision avoidance (except when necessary), in contrast to the remaining homogeneous agents (followers).
4) The proposed distributed coordination and control protocol. More specifically: on one hand, the adopted assumptions on the available sensing and communication are relevant to realistic applications such as surveillance missions, where multiple robotic agents need to collaborate towards the accomplishment of a common task under limited information. On the other hand, by adopting the necessary and sufficient conditions of Nagumo's Theorem on rendering a given set (weakly) positively invariant, we immediately have the necessary and sufficient conditions on preserving safety and connectivity w.r.t. the adopted safety and connectivity sets. Based on these conditions we provide characterizations on conflict resolution among agents (see the analysis in Appendix B), and based on these characterizations we build the proposed coordination and control protocol. In that sense, our control strategies employ levels of available information only when necessary. Furthermore, they dictate *semi-cooperative* conflict resolution among homogeneous agents (which can be also thought as prioritization), as well as conflict resolution w.r.t. an agent (the leader) which is not participating in collision avoidance.

A preliminary version of the current paper addressing mostly the objectives' encoding via our novel Lyapunov-like barrier functions appeared in [26]. Compared to the conference version, the current paper additionally includes: (i) The detailed definition of our distributed conflict resolution and motion coordination protocol, (ii) the control design for the perturbed multi-agent system, i.e., for the case when the goal destinations and connectivity region are dynamic, as well as (iii) the detailed proofs verifying the correctness of the proposed control algorithms, which where omitted in the conference submission in the interest of space.

The paper is organized as follows: Section II describes the mathematical modeling, considered assumptions and problem formulation, while Section III presents the objectives' encoding via our novel Lyapunov-like barrier functions. The motion coordination and control design is addressed in Section IV and simulation results demonstrate the efficacy of our approach in Section V. Conclusions and ideas on current and future research are summarized in Section VI. Finally, the Appendices A-D include the proofs of the Theorems 2-5.

II. Modeling and Problem Statement

Consider a network of N mobile agents with unicycle kinematics, which is deployed in a known workspace (environment) $\mathcal{W}$ with static obstacles. Each agent $i \in \{1, \ldots, N\}$ is modeled as a circular disk of radius r_a, and its motion w.r.t. a global Cartesian coordinate frame $\mathcal{G}$ is described by:

$$\dot{\boldsymbol{q}}_i = \boldsymbol{G}_i(\theta_i)\boldsymbol{\nu}_i \Rightarrow \begin{bmatrix} \dot{x}_i \\ \dot{y}_i \\ \dot{\theta}_i \end{bmatrix} = \begin{bmatrix} \cos\theta_i & 0 \\ \sin\theta_i & 0 \\ 0 & 1 \end{bmatrix} \begin{bmatrix} u_i \\ \omega_i \end{bmatrix}, \tag{1}$$

where $\boldsymbol{q}_i = \begin{bmatrix} x_i & y_i & \theta_i \end{bmatrix}^T \in \mathcal{Q}_i$ is the configuration vector of agent i, comprising the position $\boldsymbol{r}_i = \begin{bmatrix} x_i & y_i \end{bmatrix}^T \in \mathcal{R}_i$ and the orientation $\theta_i \in \mathcal{S}$ of agent i, $\mathcal{Q}_i = \mathcal{R}_i \times \mathcal{S}$ is the configuration space of agent i, and $\boldsymbol{\nu}_i = \begin{bmatrix} u_i & \omega_i \end{bmatrix}^T$ is the vector of control inputs, comprising the linear velocity u_i and the angular velocity ω_i, expressed in the body-fixed frame $\mathcal{B}_i$.

The environment $\mathcal{W}$ is populated with M static circular obstacles of known radii, which are centered at known positions $\boldsymbol{p}_m$, $m \in \{1, \ldots, M\}$. The consideration of polygonal obstacle environments is beyond the length and the scope of the current paper, while a relevant discussion is included later on in the Conclusions section.

Remark 1: The subsystem describing the evolution of the orientation trajectories $\theta_i(t)$ is linear and can be controlled using a PD controller. In this respect, the orientation θ_i can be regulated to any desired value θ_{id}, as long as the resulting angular velocity ω_i respects realistic saturation bounds (these are not explicitly considered in this paper). Such assumption is plausible for differentially-driven mobile robots, and is a key characteristic which allows to perform the time scale decomposition of the multi-agent system described later on.

We denote the leader agent as agent $i = 1$. The leader is not actively avoiding collisions with followers, and furthermore does not deviate from its nominal motion plan except if necessary, i.e., except for avoiding static obstacles. On the other hand, the followers are assigned to move towards desired destinations (convergence) while avoiding inter-agent collisions and static obstacles (safety), and while staying close enough to the leader, so that they can reliably receive information on their goal positions (connectivity maintenance).

The leader has access only to its own state, i.e., does not sense or receive any information on the states of the remaining agents and communicates information to them regarding their goal destinations. Each follower has access to its own state, measures the position of agents lying in its sensing area (realized as a circular disk of radius R_s), exchanges information on pose and velocity with agents lying in its safety area (realized as a circular disk of radius $R_c < R_s$), and receives information from the leader regarding to its goal destination as long as the leader

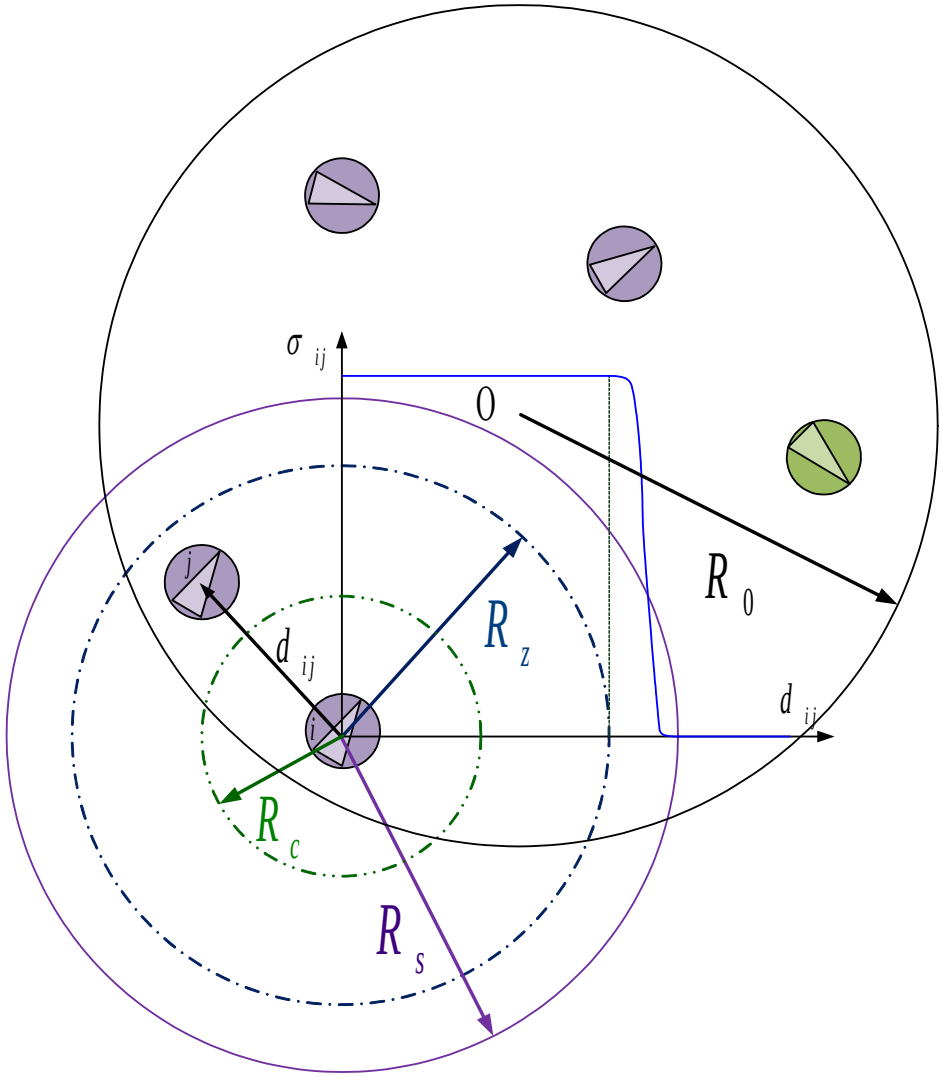

Fig. 1. The leader agent can reliably broadcast information to any follower agent lying within distance less than $2R_0$; this is realized by forcing all agents to move in a circular connectivity region O of radius R_0, centered at some point $\boldsymbol{r}_0$. Each follower agent i can measure the position $\boldsymbol{r}_j$ of any agent j lying within distance $d_{ij} \leq R_s$, i.e., within its sensing region. Furthermore, each follower agent i receives the orientation θ_j and linear velocity u_j of any agent j lying within distance $d_{ij} \leq R_c$, i.e., within its safety region. Finally, the circular region of radius R_z centered at each follower agent i denotes the region in which the collision avoidance objective is active for agent i, see the detailed analysis in Section III-B.

lies within a known upper bounded distance w.r.t. the follower. This requirement is ensured if all N agents remain within a circular region O centered at $\boldsymbol{r}_0 = \begin{bmatrix} x_0 & y_0 \end{bmatrix}^T$ and of radius R_0, see also Fig. 1. The transmission of goal destinations from the leader to the followers does not need to be in a synchronous mode, i.e., the followers' goal destinations are not necessarily updated at the same time. Finally, all agents move in a cooperative fashion, i.e., they are rational and do not behave in a malicious way.

In the next section, we describe how these diverse objectives and sensing/communication patterns can be encoded

via single Lyapunov-like barrier functions for each one of the agents.

III. Encoding objectives via Lyapunov-like barrier functions

In constrained optimization, a barrier function is a continuous function whose value on a point increases to infinity as the point approaches the boundary of the feasible region; therefore, a barrier function is used as a penalizing term for violations of constraints. The concept of *recentered barrier functions* in particular was introduced in [24] in order to not only regulate the solution to lie in the interior of the constrained set, but also to ensure that, if the system converges, then it converges to a desired point.

A. Connectivity maintenance

Any follower can reliably receive information from the leader as long as the distance between them remains less or equal than a maximum distance $2R_0$. This requirement can be ensured if all N agents remain within a circular region O centered at $\boldsymbol{r}_0 = \begin{bmatrix} x_0 & y_0 \end{bmatrix}^T$ and of radius R_0 as shown in Fig. 1, or in other words, if the distance $d_{i0} = \|\boldsymbol{r}_i - \boldsymbol{r}_0\|$ remains always less or equal than $R = R_0 - r_a$, which reads:

$$c_{i0} = R - \|\boldsymbol{r}_i - \boldsymbol{r}_0\| \geq 0. \tag{2}$$

The inequality (2) is a nonlinear inequality constraint which should never be violated. In the sequel, for all $i \in \{1, \ldots, N\}$ we refer to the N constraints (2) as to *proximity* constraints. The constrained set encoding the circular region O, or the connectivity region, for each agent i is denoted as $\mathcal{K}_{i0} = \{\boldsymbol{r}_i \in \mathcal{R}_i \mid c_{i0}(\boldsymbol{r}_i) \geq 0\}$.[1] Connectivity for the robotic network is then maintained as long as the constraints (2) hold for all $i \in \{1, \ldots, N\}$.

Inspired in part by interior point methods [27], we define the logarithmic barrier function[2] $b_{i0}(\boldsymbol{r}_i) : \mathcal{R}_i \to \mathbb{R}$ of the constraint $c_{i0}(\boldsymbol{r}_i)$ as:

$$b_{i0}(\boldsymbol{r}_i) = -\ln\left(c_{i0}(\boldsymbol{r}_i)\right),$$

which tends to $+\infty$ as $c_{i0}(\boldsymbol{r}_i) \to 0$. Then, the *gradient recentered barrier function* for the constraint $c_{i0}(\boldsymbol{r}_i)$ is defined as [24]:

$$r_{i0}(\boldsymbol{r}_i) = b_{i0}(\boldsymbol{r}_i) - b_{i0}(\boldsymbol{r}_{id}) - \left(\nabla b_{i0}\big|_{\boldsymbol{r}_{id}}\right)^T (\boldsymbol{r}_i - \boldsymbol{r}_{id}), \tag{3}$$

where $\boldsymbol{r}_{id} = \begin{bmatrix} x_{id} & y_{id} \end{bmatrix}^T$ is the goal position of agent i, $\nabla b_{i0} = \begin{bmatrix} \frac{\partial b_{i0}}{\partial x_i} & \frac{\partial b_{i0}}{\partial y_i} \end{bmatrix}^T$ is the gradient (column) vector of the function $b_{i0}(\boldsymbol{r}_i)$, and $\left(\nabla b_{i0}\big|_{\boldsymbol{r}_{id}}\right)^T$ is the transpose of this gradient vector (i.e., is a row vector, for the dimensions to match) *evaluated at the goal position* $\boldsymbol{r}_{id}$. Note that the analytical expression of the gradient vector

[1]Note that requiring all agents to remain within a region may also be desirable for ensuring that the group avoids (static) physical obstacles.

[2]The choice of the logarithmic barrier function is not restrictive; one may use other types of barriers, e.g., the inverse barrier function $b_{ij} = \frac{1}{c_{ij}}$.

is $\nabla b_{i0} = \frac{1}{\|\boldsymbol{r}_i - \boldsymbol{r}_0\|(R - \|\boldsymbol{r}_i - \boldsymbol{r}_0\|)}(\boldsymbol{r}_i - \boldsymbol{r}_0)$ and therefore we take $\boldsymbol{r}_{id} \neq \boldsymbol{r}_0$ and $\|\boldsymbol{r}_{id} - \boldsymbol{r}_0\| \neq R$, so that $\nabla b_{i0}\big|_{\boldsymbol{r}_{id}}$ is always well-defined.[3]

The recentered barrier function (3): (i) is zero at the goal position $\boldsymbol{r}_{id}$ of agent i, and (ii) tends to $+\infty$ as $c_{i0}(\boldsymbol{r}_i) \to 0$, i.e., as the position $\boldsymbol{r}_i$ of agent i approaches the boundary of the constrained set $\mathcal{K}_{i0}$. Motivated by these characteristics, the main idea here is to employ (3) in order to encode *both* connectivity maintenance (i.e., staying within the connectivity region) *and* convergence to a goal position $\boldsymbol{r}_{id}$ for each agent $i \in \{1, \ldots, N\}$. In order to ensure that we have an everywhere nonnegative function encoding these objectives so that it can be used in Lyapunov-like control design and analysis as in [25], we define the function $V_{i0} : \mathcal{R}_i \to \mathbb{R}^+$ as:

$$V_{i0}(\boldsymbol{r}_i) = (r_{i0}(\boldsymbol{r}_i))^2 . \tag{4}$$

At this point let us state the following lemma, which is useful for the analysis later on.

Lemma 1: The recentered barrier function (3) vanishes only at the goal position $\boldsymbol{r}_{id}$. Consequently, the function V_{i0} given by (4) is positive definite w.r.t. the goal position $\boldsymbol{r}_{id}$.

Proof: Assume the existence of a point $\boldsymbol{r}_{id}^\star \neq \boldsymbol{r}_{id}$ which is a solution of (3). Then:

$$b_{i0}(\boldsymbol{r}_{id}^\star) - b_{i0}(\boldsymbol{r}_{id}) - \left(\nabla b_{i0}\big|_{\boldsymbol{r}_{id}}\right)^T (\boldsymbol{r}_{id}^\star - \boldsymbol{r}_{id}) = 0, \tag{5}$$

where:

$$b_{i0}(\boldsymbol{r}_{id}^\star) = -\log(R - \|\boldsymbol{r}_{id}^\star - \boldsymbol{r}_0\|), \tag{6a}$$

$$b_{i0}(\boldsymbol{r}_{id}) = -\log(R - \|\boldsymbol{r}_{id} - \boldsymbol{r}_0\|), \tag{6b}$$

$$\nabla b_{i0}\big|_{\boldsymbol{r}_{id}} = \frac{1}{\|\boldsymbol{r}_{id} - \boldsymbol{r}_0\| \left(R - \|\boldsymbol{r}_{id} - \boldsymbol{r}_0\|\right)} \left(\boldsymbol{r}_{id} - \boldsymbol{r}_0\right), \tag{6c}$$

and by definition: $\|\boldsymbol{r}_{id} - \boldsymbol{r}_0\| \neq 0$, $\|\boldsymbol{r}_{id} - \boldsymbol{r}_0\| \neq R$. To further simplify the notation, let us denote:

$$\boldsymbol{r}_{id} = \boldsymbol{r}_0 + \mathbf{x} \Rightarrow \mathbf{x} = \boldsymbol{r}_{id} - \boldsymbol{r}_0, \tag{7a}$$

$$\boldsymbol{r}_{id}^\star = \boldsymbol{r}_0 + \mathbf{y} \Rightarrow \mathbf{y} = \boldsymbol{r}_{id}^\star - \boldsymbol{r}_0, \tag{7b}$$

$$\boldsymbol{r}_{id}^\star = \boldsymbol{r}_{id} + \mathbf{z} \Rightarrow \mathbf{z} = \boldsymbol{r}_{id}^\star - \boldsymbol{r}_{id}. \tag{7c}$$

[3]This physically means that the goal position $\boldsymbol{r}_{id}$ can lie neither on the center, nor on the boundary of the connectivity region O, an assumption which is not restrictive from a practical point of view.

Substituting (6) and (7) into (5) yields:

$$
\begin{aligned}
-\log(R-\|\mathbf{y}\|)+\log(R-\|\mathbf{x}\|)-\frac{\mathbf{x}^T\mathbf{z}}{\|\mathbf{x}\|\,(R-\|\mathbf{x}\|)}=0 \Rightarrow \\
\log(R-\|\mathbf{y}\|)-\log(R-\|\mathbf{x}\|)+\frac{\mathbf{x}^T\mathbf{z}}{\|\mathbf{x}\|\,(R-\|\mathbf{x}\|)}=0 \Rightarrow \\
\log\left(\frac{R-\|\mathbf{y}\|}{R-\|\mathbf{x}\|}\right)+\frac{\mathbf{x}^T(\mathbf{y}-\mathbf{x})}{\|\mathbf{x}\|\,(R-\|\mathbf{x}\|)}=0 \Rightarrow \\
\log\left(\frac{R-\|\mathbf{y}\|}{R-\|\mathbf{x}\|}\right)+\frac{\|\mathbf{x}\|\|\mathbf{y}\|\cos\beta-\|\mathbf{x}\|^2}{\|\mathbf{x}\|\,(R-\|\mathbf{x}\|)}=0 \overset{\mathbf{x}\neq\mathbf{0}}{\Rightarrow} \\
\log\left(\frac{R-\|\mathbf{y}\|}{R-\|\mathbf{x}\|}\right)+\frac{\|\mathbf{y}\|\cos\beta-\|\mathbf{x}\|}{R-\|\mathbf{x}\|}=0 \Rightarrow \\
\log\left(\frac{R-\|\mathbf{y}\|}{R-\|\mathbf{x}\|}\right)=\frac{\|\mathbf{x}\|-\|\mathbf{y}\|\cos\beta}{R-\|\mathbf{x}\|},
\end{aligned}
\tag{8}
$$

where β is the angle between vectors $\mathbf{x}$ and $\mathbf{y}$. We proceed with considering the following two cases:

1) Assume $\|\mathbf{y}\|\geq\|\mathbf{x}\|$. We can write: $\|\mathbf{y}\|=\lambda\,(R-\|\mathbf{x}\|)+\|\mathbf{x}\|$, where $\lambda\in[0,1]$. Then (8) reads:

$$
\begin{aligned}
\log\left(\frac{R-\lambda\,(R-\|\mathbf{x}\|)-\|\mathbf{x}\|}{R-\|\mathbf{x}\|}\right)= \\
=\frac{\|\mathbf{x}\|-(\lambda\,(R-\|\mathbf{x}\|)+\|\mathbf{x}\|)\cos\beta}{R-\|\mathbf{x}\|} \Rightarrow \\
\log(1-\lambda)=\frac{\|\mathbf{x}\|}{R-\|\mathbf{x}\|}-\left(\lambda+\frac{\|\mathbf{x}\|}{R-\|\mathbf{x}\|}\right)\cos\beta.
\end{aligned}
$$

Denote $\frac{\|\mathbf{x}\|}{R-\|\mathbf{x}\|}=\gamma$ to further write:

$$
\log(1-\lambda)=\gamma-(\lambda+\gamma)\cos\beta \Rightarrow \cos\beta=\frac{\gamma-\log(1-\lambda)}{\lambda+\gamma}.
$$

Since $\cos\beta\leq 1$, we have:

$$
\gamma-\log(1-\lambda)\leq\lambda+\gamma \Rightarrow \underbrace{\log(1-\lambda)+\lambda}_{g(\lambda)}\geq 0. \tag{9}
$$

Consider the equality $g(\lambda)=0$ and note that $\lambda=0$ is a solution, $g(0)=0$. Furthermore, one has $g'(\lambda)=-\frac{\lambda}{1-\lambda}<0$ for $\lambda\in(0,1]$. This implies that $g(\lambda)$ is decreasing for $\lambda\in(0,1]$, i.e., $g(\lambda)\leq 0$ for $\lambda\in[0,1]$. Consequently, (9) is true only as an equality, and furthermore the solution $\lambda=0$ of this equality is unique. Recall that $\lambda=0$ corresponds to $\|\mathbf{y}\|=\|\mathbf{x}\|$. Then out of (8): $\|\mathbf{x}\|(1-\cos\beta)\overset{\mathbf{x}\neq\mathbf{0}}{=}0\Rightarrow\cos\beta=1$. Therefore one has: $\|\mathbf{y}\|=\|\mathbf{x}\|$ and $\cos\beta=1$, which implies that $\mathbf{y}=\mathbf{x}\Rightarrow\boldsymbol{r}_{id}^{\star}=\boldsymbol{r}_{id}$.

2) Assume that $\|\mathbf{y}\|<\|\mathbf{x}\|$. We can write: $\|\mathbf{y}\|=\lambda\|\mathbf{x}\|$, where $\lambda\in(0,1)$. Then (8) reads:

$$
\begin{aligned}
\log\left(\frac{R-\lambda\|\mathbf{x}\|}{R-\|\mathbf{x}\|}\right)=\frac{\|\mathbf{x}\|(1-\lambda\cos\beta)}{R-\|\mathbf{x}\|} \Rightarrow \\
\log\left(\frac{R-\|\mathbf{x}\|+(1-\lambda)\|\mathbf{x}\|}{R-\|\mathbf{x}\|}\right)=\frac{\|\mathbf{x}\|}{R-\|\mathbf{x}\|}-\frac{\|\mathbf{x}\|\lambda\cos\beta}{R-\|\mathbf{x}\|}.
\end{aligned}
$$

Denote $\frac{\|\mathbf{x}\|}{R-\|\mathbf{x}\|} = \gamma$ to further write:

$$\log\left(1+(1-\lambda)\gamma\right) = \gamma - \gamma\lambda\cos\beta \Rightarrow$$
$$\cos\beta = \frac{\gamma - \log\left(1+(1-\lambda)\gamma\right)}{\lambda\gamma}.$$

Since $\cos\beta \leq 1$, we further have:

$$\gamma - \log(1+(1-\lambda)\gamma) \leq \lambda\gamma \Rightarrow$$
$$\underbrace{\log(1+(1-\lambda)\gamma) - (1-\lambda)\gamma}_{g(\lambda)} \geq 0. \tag{10}$$

Consider the equality $g(\lambda) = 0$ and note that $\lambda = 1$ is a solution, $g(1) = 0$. Furthermore, one has $g'(\lambda) = \frac{\gamma^2(1-\lambda)}{1+\gamma(1-\lambda)} > 0$ for $\lambda \in (0,1)$. This implies that $g(\lambda)$ is increasing for $\lambda \in (0,1)$, i.e., $g(\lambda) < 0$ for $\lambda \in (0,1)$. Consequently, the inequality (10) does not have any solutions for $\lambda \in (0,1)$.

In summary, one concludes that the solutions of (8) reduce to $\boldsymbol{r}_{id}^{\star} = \boldsymbol{r}_{id}$, i.e., the goal position $\boldsymbol{r}_{id}$ is the unique solution of the recentered barrier function (3). It then trivially follows that the function (4) is positive definite w.r.t. $\boldsymbol{r}_{id}$. This completes the proof. ■

B. Collision avoidance

Agent $i \in \{2,\ldots,N\}$ realizes agent $j \in \{1,\ldots,N\}$, $j \neq i$, as a physical obstacle. Therefore, agent i avoids collision with agent j as long as the distance $d_{ij} = \|\boldsymbol{r}_i - \boldsymbol{r}_j\|$ remains greater or equal than a minimum separation distance $d_s \geq 2r_a$, i.e.,:

$$c_{ij} = (x_i - x_j)^2 + (y_i - y_j)^2 - {d_s}^2 \geq 0. \tag{11}$$

In the sequel, for all $i \in \{2,\ldots,N\}$ and all $j \in \{1,\ldots,N\}$, with $j \neq i$, we refer to the resulting $(N-1)\times(N-2)$ constraints as to *collision avoidance* constraints, while the constrained set encoding the collision-free space of agent i w.r.t. agent j is denoted with $\mathcal{K}_{ij} = \{\boldsymbol{r}_i \in \mathcal{R}_i, \boldsymbol{r}_j \in \mathcal{R}_j \mid c_{ij}(\boldsymbol{r}_i,\boldsymbol{r}_j) \geq 0\}$. The logarithmic barrier function $b_{ij}(\boldsymbol{r}_i,\boldsymbol{r}_j) : \mathcal{R}_i \times \mathcal{R}_j \to \mathbb{R}$ for the constraint $c_{ij}(\boldsymbol{r}_i,\boldsymbol{r}_j)$ is defined as:

$$b_{ij}(\boldsymbol{r}_i,\boldsymbol{r}_j) = -\ln\left(c_{ij}(\boldsymbol{r}_i,\boldsymbol{r}_j)\right).$$

We consider the barrier function $q_{ij} : \mathcal{R}_i \times \mathcal{R}_j \to \mathbb{R}$ as:

$$q_{ij}(\boldsymbol{r}_i,\boldsymbol{r}_j) = b_{ij}(\boldsymbol{r}_i,\boldsymbol{r}_j) - b_{ij}(\boldsymbol{r}_{id},\boldsymbol{r}_j), \tag{12}$$

which is zero at the goal position $\boldsymbol{r}_{id}$ of agent i and tends to $+\infty$ as $c_{ij}(\boldsymbol{r}_i,\boldsymbol{r}_j) \to 0$, i.e., as the distance d_{ij} tends to the minimum separation d_s. To have an everywhere nonnegative function, we define the function $V'_{ij} : \mathcal{R}_i \times \mathcal{R}_j \to \mathbb{R}^+$ as:

$$V'_{ij}(\boldsymbol{r}_i,\boldsymbol{r}_j) = (q_{ij}(\boldsymbol{r}_i,\boldsymbol{r}_j))^2. \tag{13}$$

Let us now recall that agent i senses agent j only when the distance d_{ij} between them is less than the sensing radius $R_s > d_s$. In other words, agent i needs only locally to avoid collision with agent j. To encode this requirement, we define the bump function:

$$\sigma_{ij} = \begin{cases} 1, & \text{if } \ d_s \leq d_{ij} \leq R_z; \\ A{d_{ij}}^3 + B{d_{ij}}^2 + Cd_{ij} + D, & \text{if } \ R_z < d_{ij} < R_s; \\ 0, & \text{if } \ d_{ij} \geq R_s, \end{cases} \tag{14}$$

where the coefficients: $A = -\frac{2}{(R_z - R_s)^3}$ $B = \frac{3(R_z + R_s)}{(R_z - R_s)^3}$, $C = -\frac{6R_z R_s}{(R_z - R_s)^3}$, $D = \frac{{R_s}^2(3R_z - R_s)}{(R_z - R_s)^3}$ have been computed such that $\sigma_{ij}(\cdot)$ is a $\mathcal{C}^2$ function w.r.t. the distance d_{ij}. We then define:

$$V_{ij}(\boldsymbol{r}_i, \boldsymbol{r}_j) = \sigma_{ij} \ V'_{ij}, \tag{15}$$

with σ_{ij} given by (14) and V'_{ij} given by (13). In this way, collision avoidance w.r.t. for agent i w.r.t. agent j is encoded only within a finite zone of radius $R_z < R_s$ around agent i.

C. Barrier functions for collision avoidance, proximity and convergence objectives

The analytical construction and properties of the functions (13), (15), (4) allow for handling the collision avoidance, proximity and convergence objectives via a single Lyapunov-like function V_i for each agent i. A follower agent $i \neq 1$ has $N-1$ avoidance objectives encoded via $N-1$ functions V_{ij}, and one proximity objective encoded via function V_{i0}. Agent i needs finally to converge to goal destination $\boldsymbol{r}_{id}$; to this end, note that by construction all functions V_{in}, where $n \in \mathcal{N} = \{0, 1, \ldots, N\}$ and $n \neq i$, are zero at the goal destination $\boldsymbol{r}_{id}$. Thus, following our previous work [25], we encode the accomplishment of all objectives for agent i by an approximation of the maximum function (which also is a δ-norm when δ takes integer values), of the form:

$$v_i = \left((V_{i0})^\delta + \sum_{j=1, j\neq i}^{N} (V_{ij})^\delta \right)^{\frac{1}{\delta}} = \left(\sum_{n \in \mathcal{N}} (V_{in})^\delta \right)^{\frac{1}{\delta}}, \tag{16}$$

where $\delta \in [1, +\infty)$. The function $v_i : \mathbb{R}^{2N} \to \mathbb{R}^+$ is nonnegative everywhere in the constrained set $\mathcal{K}_i = \bigcup_{n \in \mathcal{N}} \mathcal{K}_{in}$ of agent i and tends to $+\infty$ as at least one of the terms V_{in} tends to $+\infty$, i.e., as the position $\boldsymbol{r}_i$ of agent i approaches the boundary of the constrained set $\mathcal{K}_i$. Furthermore, v_i is zero when all functions V_{in} are zero. Thus, v_i is by definition zero at the goal position $\boldsymbol{r}_{id}$.

Finally, for ensuring that all objectives are encoded by a single function which *uniformly* attains its maximum value on the boundary of the constrained set $\mathcal{K}_i$,[4] we define:

$$V_i = \frac{v_i}{1 + v_i} = \frac{\left(\sum_{n \in \mathcal{N}} (V_{in})^\delta \right)^{\frac{1}{\delta}}}{1 + \left(\sum_{n \in \mathcal{N}} (V_{in})^\delta \right)^{\frac{1}{\delta}}}, \tag{17}$$

which is zero for $v_i = 0$, i.e., at the goal position $\boldsymbol{r}_{id}$ of agent i, and equal to 1 as $v_i \to +\infty$, i.e., on the boundary of the constrained set $\mathcal{K}_i$. We can now state the following Theorem.

[4]The reason for requiring this property is justified in Lemma 3.

Theorem 1: The Lyapunov-like function (17) is positive definite w.r.t. the goal position $\boldsymbol{r}_{id}$.

Proof: Since the function $f(\kappa) = \frac{\kappa}{1+\kappa}$ is monotonically increasing for $\kappa \in [0, +\infty)$, it suffices to prove that (16) is positive definite w.r.t. the goal position $\boldsymbol{r}_{id}$. Out of Lemma 1 one has that the function V_{i0} given by (4) is positive definite w.r.t. $\boldsymbol{r}_{id}$. This trivially implies that (16) is positive definite w.r.t. $\boldsymbol{r}_{id}$ as well; to see why, consider that if $\boldsymbol{r}^{\star}_{id} \neq \boldsymbol{r}_{id}$ were a solution of (16), then it would hold that $V_{in}(\boldsymbol{r}^{\star}_{id}) = 0,\ \forall n \in \{0, 1, \ldots, N\}$ with $n \neq i$, i.e., it would hold that $V_{i0}(\boldsymbol{r}^{\star}_{id}) = 0$, which is a contradiction since (4) is positive definite w.r.t. $\boldsymbol{r}_{id}$. ■

Remark 2: One of the merits of the analytical construction of (17) is that it may easily incorporate collision avoidance of agent i w.r.t. all or just a subset of agents $j \neq i$, i.e., one may take into account the "neighbor agents" j in (17) according to given communication topologies.

IV. Motion Coordination

All agents initiate in the region O, so that reliable wireless communication links can be established. The leader $j = 1$ communicates a goal position $\boldsymbol{r}_{jd}$ to each follower $j \neq 1$ and moves towards its goal destination $\boldsymbol{r}_{1d}$; however, the leader is not actively trying to avoid any follower throughout its motion towards $\boldsymbol{r}_{1d}$. Each follower $j \neq 1$ needs to navigate towards, and remain close to, its goal destination $\boldsymbol{r}_{jd}$, while avoiding the leader and other followers, and while remaining connected with the leader. The pairwise distance between goal destinations is assumed to be $\|\boldsymbol{r}_{jd} - \boldsymbol{r}_{kd}\| > 2\ R_s$, $\forall (j, k)$ so that each agent j does not sense any other goal destination $\boldsymbol{r}_{kd}$ when already at $\boldsymbol{r}_{jd}$. We assume for now that:

1) The goal positions $\boldsymbol{r}_{jd}$, $j \in \{1, \ldots, N\}$ and the center $\boldsymbol{r}_0$ of the region O are static, which yields: $\frac{d}{dt}\boldsymbol{r}_{jd} = \boldsymbol{0}$ and $\frac{d}{dt}\boldsymbol{r}_0 = \boldsymbol{0}$, respectively. In this case we refer to the multi-robot system as to the nominal system.
2) There are no physical obstacles in the region O.

A. Motion Coordination for the Nominal System

1) Control laws for agent $j = 1$:

Theorem 2: The position trajectories $\boldsymbol{r}_1(t)$ of the leader starting in the interior of the connectivity region are asymptotically stable to the goal destination $\boldsymbol{r}_{1d}$ and always remain in the connectivity region under:

$$u_1 = k_1 \tanh(\|\boldsymbol{r}_1 - \boldsymbol{r}_{1d}\|), \tag{18a}$$

$$\omega_1 = -\lambda_1(\theta_1 - \phi_1) + \dot{\phi}_1, \tag{18b}$$

where V_1 is the Lyapunov-like function (17) for $n = 0$, $\delta \geq 1$, $\phi_1 \triangleq \operatorname{atan2}\left(-\frac{\partial V_1}{\partial y_1}, -\frac{\partial V_1}{\partial x_1}\right)$, and $k_1,\ \lambda_1 > 0$. The proof is given in the Appendix A.

2) Control laws for agents $j \in \{2, \ldots, N\}$:

Theorem 3: Each agent $j \in \{2, \ldots, N\}$ converges almost surely to its goal destination while avoiding collisions

and while remaining in the connectivity region under:

$$u_j = \begin{cases} \min_{i\in\mathcal{I}|J_i<0} u_{j|i}, & d_s \le d_{ji} \le R_c, \\ u_{jc}, & R_c < d_{ji}; \end{cases}, \tag{19a}$$

$$\omega_j = -\lambda_j(\theta_j - \phi_j) + \dot{\phi}_j, \tag{19b}$$

where: $\mathcal{I} \in \{k, l, m, \dots\}$ the set of agents in the safety region of agent j, $J_i = \boldsymbol{r}_{ij}{}^T \begin{bmatrix} \cos\phi_j \\ \sin\phi_j \end{bmatrix}$, $\boldsymbol{r}_{ij} = \boldsymbol{r}_j - \boldsymbol{r}_i$, $d_{ij} = \|\boldsymbol{r}_{ij}\|$,

$$u_{j|i} = u_{jc}\frac{d_{ij} - d_s}{R_c - d_s} + u_{js|i}\frac{R_c - d_{ij}}{R_c - d_s},$$

$$u_{jc} = k_j \tanh\left(\|\boldsymbol{r}_j - \boldsymbol{r}_{jd}\|\right), \quad u_{js|i} = u_i \frac{\boldsymbol{r}_{ij}{}^T\boldsymbol{\eta}_i}{\boldsymbol{r}_{ij}{}^T\boldsymbol{\eta}_j},$$

$\boldsymbol{\eta}_j = \begin{bmatrix} \cos\phi_j \\ \sin\phi_j \end{bmatrix}$, $\phi_j \triangleq \operatorname{atan2}\left(-\frac{\partial V_j}{\partial y_j}, -\frac{\partial V_j}{\partial x_j}\right)$, $\delta \ge 1$ and $k_j,\ \lambda_j > 0$. The proof is given in the Appendix B.

Remark 3: Let us now assume that the connectivity region O is populated with M static circular obstacles centered at positions $\boldsymbol{p}_m$, $m \in \{1, \dots, M\}$. Obstacle avoidance for agent $i \in \{1, \dots, N\}$ can then be encoded by incorporating M barrier functions of the form (15) into the Lyapunov-like function (16). In this case, the analysis regarding to the collision-free and connectivity preserving motion of the followers' is similar with the one in Theorem 3. The only difference lies in the analysis regarding to the convergence to their goal destinations, since the squared recentered barrier functions introduce additional critical points in the Lyapunov-like function V_j. Similarly, the convergence of the leader becomes almost sure, since at least M saddle points are introduced in the Lyapunov-like function V_1.

B. Motion Coordination for the Perturbed System

So far we assumed that $\frac{d}{dt}\boldsymbol{r}_0 = \boldsymbol{0}$ and $\frac{d}{dt}\boldsymbol{r}_{jd} = \boldsymbol{0}$, i.e., that the agents operate in a static connectivity region and need to converge to static goal destinations. Let us now consider the perturbed system, i.e., the case when the leader moves with some linear velocity $k_1 \neq 0$ and updates the destinations $\boldsymbol{r}_{jd}$ and the center $\boldsymbol{r}_0$ so that $\|\frac{d}{dt}\boldsymbol{r}_0\| \le k_d$, $\|\frac{d}{dt}\boldsymbol{r}_{jd}\| \le k_d$.

Theorem 4: The position trajectories $\boldsymbol{r}_1(t)$ of the leader never escape the connectivity region O and are locally asymptotically stable w.r.t. the dynamic goal destination $\boldsymbol{r}_{1d}$, varying so that $\|\frac{d}{dt}\boldsymbol{r}_{1d}\| \le k_d$, under the control law:

$$u_1 = k_1, \tag{20a}$$

$$\omega_1 = -\lambda_1(\theta_1 - \phi_1) + \dot{\phi}_1, \tag{20b}$$

where ϕ_1 is defined as in Theorem 2, V_1 is the Lyapunov-like function (17) for $j = 0$, $\delta \ge 1$ and $k_1 > 2k_d > 0$, $\lambda_1 > 0$. The proof is given in the Appendix C.

Finally, let us consider the motion of the followers when the goal destinations $\boldsymbol{r}_{jd}$ and the center $\boldsymbol{r}_0$ of the connectivity region are updated by the leader so that $\|\frac{d}{dt}\boldsymbol{r}_0\| \le k_d$, $\|\frac{d}{dt}\boldsymbol{r}_{jd}\| \le k_d$.

Theorem 5: Each agent $j \in \{2, \ldots, N\}$ converges almost surely to its dynamic goal destination $\boldsymbol{r}_{jd}$, while avoiding collisions w.r.t. agents $k \neq j$ and while remaining in the connectivity region under the control law as defined in Theorem 3. The proof is given in the Appendix D.

V. Simulations

The efficacy of the proposed control algorithms is demonstrated through some representative computer simulations.

We consider a scenario of $N = 14$ agents in the operating environment. All agents are of radius $r_a = 0.5$ m and initiate in the connectivity region O, which is of radius $R_0 = 12$ m and initially centered at $\boldsymbol{r}_0 = [-3 \;\; 0]^T$. Each agent needs to move to its destination $\boldsymbol{r}_{id} \in O$, depicted in the same color as shown in Fig. 2. Agent $i = 1$ is the leader, i.e., does not receive any information on the followers' states, nor takes into account their motion. The sensing radius and the safety radius for each follower are set equal to $R_s = 1.9$ m and $R_c = 1.6875$ m, respectively, while the parameter δ is set equal to 1. The linear velocity gains k_i are randomly selected for each agent such that $k_i \in [2.25, 4.8]$, while the angular velocity gain λ_i is set the same for all agents, $\lambda_i = 2$. This choice is to demonstrate that the algorithm works efficiently despite the fact that $k_i > \lambda_i$, i.e., that the time-scale decomposition adopted in the analysis is not restrictive from a practical point of view.

We consider the perturbed system, i.e., the case when the connectivity region and the goal destinations are moving with $k_d = 0.225$ m/sec, while the leader moves with constant linear velocity $k_1 = 2.25$ m/sec and updates the goal positions of the followers'. All agents converge to their (dynamic) goal destinations, while always remaining in the connectivity region, depicted as the external black circle. Snapshots of the agents' positions throughout the duration of the simulation are provided in Fig. 2, 3. It is noteworthy that the proposed coordination protocol manages to produce collision-free trajectories even when the agents get congested, see for instance Fig. 2(c) through Fig. 2(h), and at the same time allows agents to move in very close proximity. This is also demonstrated through the evolution of the pairwise inter-agent distances over time, which is illustrated in Fig. 4: none of the pairs of agents approaches closer than the minimum distance d_s, illustrated as the red line. Furthermore, note that followers in conflict with the leader move aside so that the leader goes through and does not deviate from its nominal trajectory. At simulation time $t = 15$ sec the leader updates some of the followers' goal destinations; this could be, for instance, so that the group avoids newly detected static obstacles, or passes through narrow corridors. The motion of the followers towards their new destinations is depicted in Fig. 3. Finally, the evolution of the inter-agent distances $d_{ij}(t)$ during the entire simulation time interval $[0, 20]$ sec is depicted in Fig. 4. The inter-agent distances remain strictly greater than $2r_a$, which verifies that collisions are avoided.

VI. Conclusions

This paper presented a set-theoretic formulation for multi-objective control problems encountered in the motion coordination of multiple agents and introduced a novel class of Lyapunov-like barrier functions to encode the agents' constrained sets. The proposed Lyapunov-like functions encode objectives such as collision avoidance, proximity

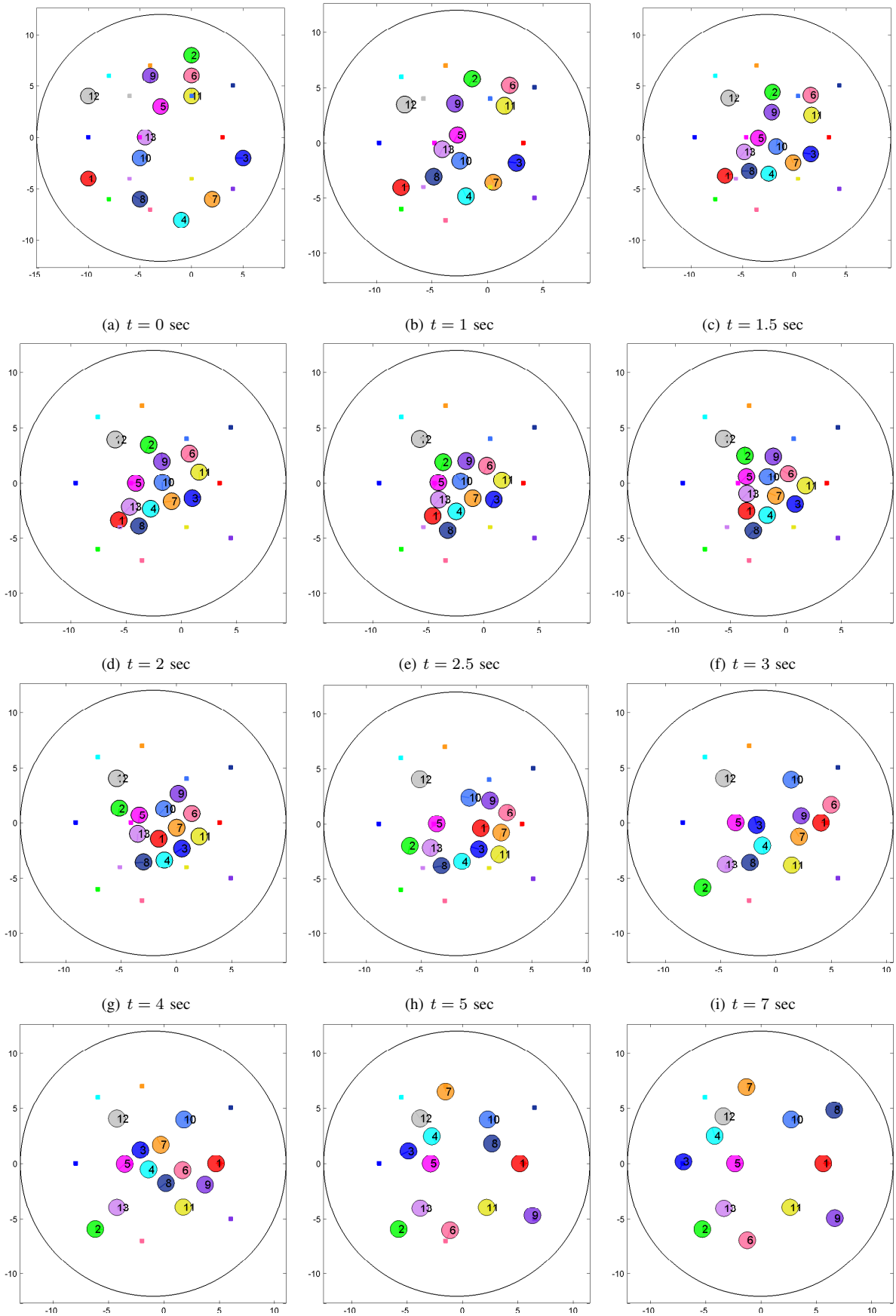

(a) $t = 0$ sec (b) $t = 1$ sec (c) $t = 1.5$ sec

(d) $t = 2$ sec (e) $t = 2.5$ sec (f) $t = 3$ sec

(g) $t = 4$ sec (h) $t = 5$ sec (i) $t = 7$ sec

(j) $t = 9$ sec (k) $t = 11$ sec (l) $t = 13$ sec

Fig. 2. The motion of the robotic group in the case that the goal destinations and the connectivity region are dynamic.

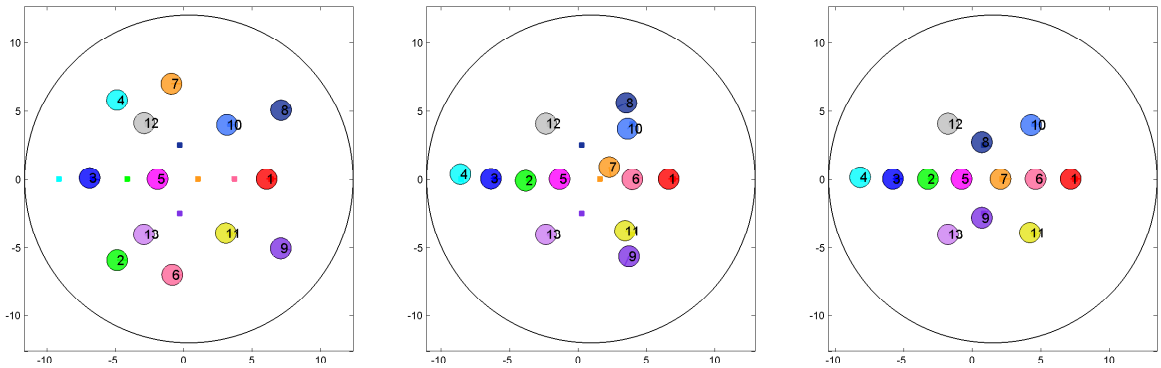

(a) $t = 15$ sec (b) $t = 17.5$ sec (c) $t = 20$ sec

Fig. 3. The motion of the robotic group in the case that the goal destinations and the connectivity region are dynamic.

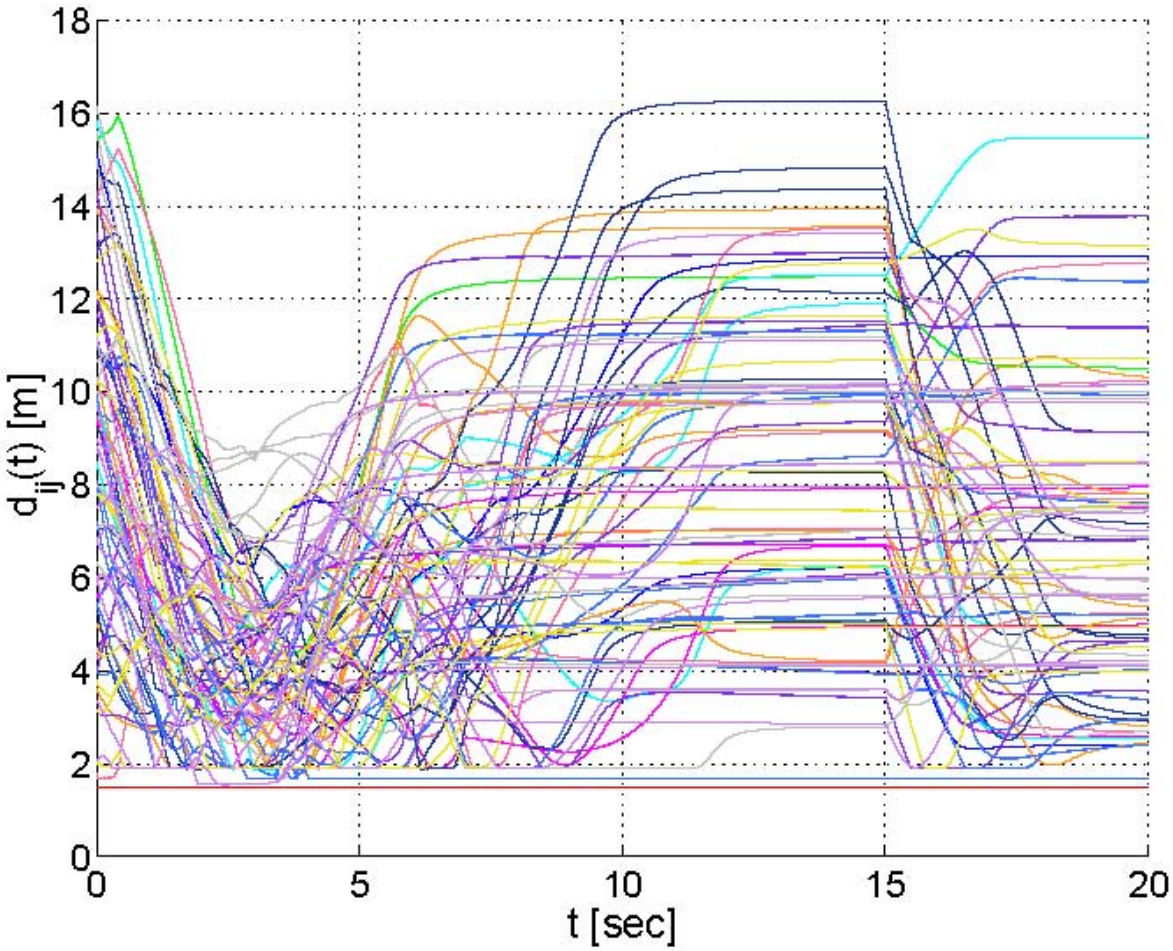

Fig. 4. The evolution of the inter-agent distances $d_{ij}(t)$.

and convergence to desired destinations, and are amenable to distributed control formulations and Lyapunov-based control design and analysis. As a consequence, one may derive gradient-based control solutions using information locally available to each agent.

The adopted assumptions on the agents' modeling are implementable on realistic robotic setups such as differentially-driven mobile robots, since the only requirement implied by the adopted time scale decomposition is to be able to control the orientation trajectories to desired values via PD controllers. The assumptions on limited sensing and communication for each agent are also relevant to standard setups such as sonars, omnidirectional cameras, laser scanners and wireless networks. Furthermore, the analysis on circular obstacles directly extends to ellipsoidal obstacles as well. When polygonal obstacles are of interest, one may define recentered barrier functions for the linear constraint functions encoding the faces of obstacles. Providing a rigorous analysis and guarantees for this case is beyond the scope and the length of the current paper. For a relevant treatment see for instance [28]. Another way of using the proposed approach in a polygonal obstacle environment is to combine the current results with those in [22]. To see how, the idea is that any follower robot of radius R_0 in the sense defined in [22] can be substituted by a group of (smaller) robots confined within a circular region of radius R_0, in the spirit presented here. This furthermore justifies the use of the circular connectivity region as a means of not only establishing reliable communications, but also of avoiding static obstacles in complex environments. The efficacy of the approach and its relevance to surveillance missions using multiple nonholonomic vehicles is illustrated via simulations. Our current work focuses on the use of Lyapunov-like barrier functions to encode vision-based sensing constraints which are pertinent to surveillance and coverage problems with robotic vehicles, and also on the consideration of agents of more complex dynamics and input constraints, such as aerial and marine robotic vehicles.

APPENDIX A
PROOF OF THEOREM 2

Proof: The required objectives for agent 1 are encoded via the Lyapunov-like function V_1 taken out of (17) for $\delta = 1$ and $n = 0$. The gradient ∇V_1 is defined everywhere in the constrained set $\mathcal{K}_1$ except for on the boundary $\partial\mathcal{K}_1$ and on the singleton $\{\boldsymbol{r}_0\}$. Denote $\Gamma = \partial\mathcal{K}_1 \bigcup \{\boldsymbol{r}_0\}$. Away from Γ, the time derivative $\dot{V}_1$ along the trajectories of agent 1 reads:

$$\dot{V}_1 = \begin{bmatrix} \frac{\partial V_1}{\partial x_1} & \frac{\partial V_1}{\partial y_1} \end{bmatrix} \begin{bmatrix} \dot{x}_1 \\ \dot{y}_1 \end{bmatrix} = \left(\frac{\partial V_1}{\partial x_1} \cos\theta_1 + \frac{\partial V_1}{\partial y_1} \sin\theta_1 \right) u_1,$$

since by construction one has $\frac{\partial V_1}{\partial \theta_1} = 0$. Substituting the control law (18a) yields:

$$\dot{V}_1 = k_1 \left(\frac{\partial V_1}{\partial x_1} \cos\theta_1 + \frac{\partial V_1}{\partial y_1} \sin\theta_1 \right) \tanh(\|\boldsymbol{r}_1 - \boldsymbol{r}_{1d}\|).$$

To keep notation compact, denote the gradient vector $\boldsymbol{\zeta}_1 \triangleq \begin{bmatrix} \frac{\partial V_1}{\partial x_1} & \frac{\partial V_1}{\partial y_1} \end{bmatrix}^T$ and define $\phi_1 \triangleq \operatorname{atan2}\left(-\frac{\partial V_1}{\partial y_1}, -\frac{\partial V_1}{\partial x_1}\right)$ as the orientation of the negated gradient $-\boldsymbol{\zeta}_1$ away from Γ. Then:

$$\frac{\partial V_1}{\partial x_1} = -\|\boldsymbol{\zeta}_1\| \cos\phi_1, \quad \frac{\partial V_1}{\partial y_1} = -\|\boldsymbol{\zeta}_1\| \sin\phi_1. \tag{21}$$

Let us at this point assume that the orientation trajectories $\theta_1(t)$ are controlled at a much faster time-scale compared to the position trajectories $\boldsymbol{r}_1(t)$. This can be realized by decomposing the agent dynamics into the boundary-layer (fast) subsystem, which describes the evolution of the orientation trajectories $\theta_1(t)$, and the reduced-layer (slow) subsystem, which describes the evolution of the position trajectories $\boldsymbol{r}_1(t)$. One may easily verify that under the control law (18b) the roots $\theta_1 = \phi_1$ are globally exponentially stable equilibria for the boundary-layer subsystem.[5]

Thus, the time derivative of the Lyapunov-like function V_1 for the reduced system, *evaluated at the roots of the boundary-layer subsystem* reads:

$$\begin{aligned}\dot{V}_1 &\overset{(21)}{=} -k_1 \left(\|\boldsymbol{\zeta}_1\| \cos^2 \phi_1 + \|\boldsymbol{\zeta}_1\| \sin^2 \phi_1\right) \tanh(\|\boldsymbol{r}_1 - \boldsymbol{r}_{1d}\|) \\ &= -k_1 \, \|\boldsymbol{\zeta}_1\| \, \tanh(\|\boldsymbol{r}_1 - \boldsymbol{r}_{1d}\|). \end{aligned} \tag{22}$$

Thus, away from Γ, $\dot{V}_1$ vanishes at the goal destination $\boldsymbol{r}_{1d}$ as well as at the points where $\boldsymbol{\zeta}_1 = \mathbf{0}$. The analytical expression for V_1 yields that the gradient vector $\boldsymbol{\zeta}_1$ vanishes at the critical points of the function V_{10}, i.e., at the positions where the gradient vector ∇V_{10} vanishes. The gradient of the function V_{10} is written analytically as: $\nabla V_{10} = 2 r_{10} \nabla r_{10}$, which implies that $\nabla V_{10} = \mathbf{0}$ at the goal position $\boldsymbol{r}_{1d}$ and at the critical points of the recentered barrier function r_{10}. One has that $\nabla r_{10} = \mathbf{0}$ at the points $\bar{\boldsymbol{r}}_{\mathbf{1}} = \begin{bmatrix} \bar{x}_1 & \bar{y}_1 \end{bmatrix}^T$, where:

$$\frac{\bar{x}_1 - x_0}{\|\bar{\boldsymbol{r}}_{\mathbf{1}} - \boldsymbol{r}_0\|(R - \|\bar{\boldsymbol{r}}_{\mathbf{1}} - \boldsymbol{r}_0\|)} = \frac{x_{1d} - x_0}{\|\boldsymbol{r}_{1d} - \boldsymbol{r}_0\|(R - \|\boldsymbol{r}_{1d} - \boldsymbol{r}_0\|)}, \tag{23a}$$

$$\frac{\bar{y}_1 - y_0}{\|\bar{\boldsymbol{r}}_{\mathbf{1}} - \boldsymbol{r}_0\|(R - \|\bar{\boldsymbol{r}}_{\mathbf{1}} - \boldsymbol{r}_0\|)} = \frac{y_{1d} - y_0}{\|\boldsymbol{r}_{1d} - \boldsymbol{r}_0\|(R - \|\boldsymbol{r}_{1d} - \boldsymbol{r}_0\|)}. \tag{23b}$$

The gradient vector ∇r_{10} is not defined on Γ. After some algebraic manipulations and away from Γ we obtain:

$$\begin{aligned}(\bar{x}_1 - x_0)^2 + (\bar{y}_1 - y_0)^2 &\overset{(23)}{=} \frac{\|\bar{\boldsymbol{r}}_{\mathbf{1}} - \boldsymbol{r}_0\|^2 (R - \|\bar{\boldsymbol{r}}_{\mathbf{1}} - \boldsymbol{r}_0\|)^2}{(R - \|\boldsymbol{r}_{1d} - \boldsymbol{r}_0\|)^2} \Rightarrow \\ \|\bar{\boldsymbol{r}}_{\mathbf{1}} - \boldsymbol{r}_0\|^2 &= \frac{\|\bar{\boldsymbol{r}}_{\mathbf{1}} - \boldsymbol{r}_0\|^2 (R - \|\bar{\boldsymbol{r}}_{\mathbf{1}} - \boldsymbol{r}_0\|)^2}{(R - \|\boldsymbol{r}_{1d} - \boldsymbol{r}_0\|)^2}, \end{aligned}$$

which is true for $\bar{\boldsymbol{r}}_{\mathbf{1}} = \boldsymbol{r}_{1d}$, i.e., the unique critical point of V_1 in $\mathcal{K}_1 \setminus \Gamma$ reduces to the goal position $\boldsymbol{r}_{1d}$. Note also that V_1 has compact level sets, and that $\dot{V}_1 \leq 0$ everywhere on $\mathcal{K}_1 \setminus \Gamma$. To be able to examine the behavior of the system solutions on Γ we employ the notion of the Clarke generalized gradient. In general, the Clarke generalized gradient of a function $f(p)$ at a point $p_\psi \in \Psi$ is defined as:

$$\partial f(p_\psi) = \mathrm{co}\{\lim_{\chi \to +\infty} \nabla f(p_\chi) : p_\chi \to p_\psi, p_\chi \notin \Psi\},$$

where Ψ is any set of measure zero where the gradient ∇f is not defined. In our case, the definition of Clarke generalized gradient of the function V_1 at a point $\boldsymbol{r}_\gamma \in \Gamma$, reduces to: $\partial V_1(\boldsymbol{r}_\gamma) = \mathrm{co}\{\lim_{\beta \to +\infty} \nabla V_1(\boldsymbol{r}_\beta) : \boldsymbol{r}_\beta \to \boldsymbol{r}_\gamma, \boldsymbol{r}_\beta \notin \Gamma\}$, where $\Gamma = \partial \mathcal{K}_1 \bigcup \{\boldsymbol{r}_0\}$. Let us first consider the set $\Gamma_1 = \partial \mathcal{K}_1$, that is, the circle O defining the connectivity region. Γ_1 can be seen as a switching surface with the gradient being equal to ∇V_1 on the interior of the set $\mathcal{K}_1$ and zero on the exterior of $\mathcal{K}_1$. Thus the generalized gradient $\partial V_1(\boldsymbol{r}_{\gamma_1})$ on the points $\boldsymbol{r}_{\gamma_1} \in \Gamma_1$ reduces to the

[5]The analysis follows the pattern used in Lemma 2 and is omitted here in the interest of space.

convex combination of the gradients on both sides of surface Γ_1, that is, $\partial V_1(\boldsymbol{r}_{\gamma_1}) = \alpha \nabla V_1 + (1-\alpha)\cdot 0 = \alpha \nabla V_1$, where $\alpha \in [0,1]$. The generalized derivative on Γ_1 for the closed-loop system dynamics is consequently defined as

$$\dot{\tilde{V}}_1(\boldsymbol{r}_{\gamma_1}) = \alpha \nabla V_1 \left(\beta \begin{bmatrix} u_1 \cos\phi_1 \\ u_1 \sin\phi_1 \end{bmatrix} + (1-\beta)\cdot 0 \right),$$

where $b \in [0,1]$ and $u_1 \geq 0$ by definition of the linear control law (18a), and further reads:

$$\dot{\tilde{V}}_1(\boldsymbol{r}_{\gamma_1}) = \alpha\beta u_1 \nabla V_1 \left(\frac{-(\nabla V_1)^T}{\|\nabla V_1\|} \right) = -\alpha\beta u_1 \|\nabla V_1\|,$$

with the norm $\|\nabla V_1\|$ and the linear velocity u_1 vanishing only at $\boldsymbol{r}_{1d}$. Let us know consider the set $\Gamma_2 = \{\boldsymbol{r}_0\}$. The generalized derivative $\dot{\tilde{V}}(\boldsymbol{r}_0)$ is then equal to

$$\mathrm{co}\left\{ \lim_{\boldsymbol{r}_1 \to \boldsymbol{r}_0} \nabla V_1(\boldsymbol{r}_1) \right\} \mathrm{co}\left\{ \lim_{\boldsymbol{r}_1 \to \boldsymbol{r}_0} u_1 \left(\frac{-(\nabla V_1(\boldsymbol{r}_1))^T}{\|\nabla V_1(\boldsymbol{r}_1)\|} \right) \right\} =$$
$$= u_1 \, \nabla V_1 \left(-\frac{\nabla V_1{}^T}{\|\nabla V_1\|} \right) = -u_1 \, \|\nabla V_1\| \leq 0,$$

with u_1, ∇V_1 vanishing at $\boldsymbol{r}_{1d}$ only. Thus, one has that the generalized derivative $\dot{\tilde{V}}(\boldsymbol{r}_1(t))$ along the system trajectories is non-positive everywhere on $\mathcal{K}_1$ and furthermore that it vanishes either at the goal position $\{\boldsymbol{r}_{1d}\}$, and on the boundary $\mathcal{K}_1$ (for $\alpha = 0$ or $\beta = 0$). Setting $\alpha = 0$ implies that the generalized gradient vector is zero; then the orientation ϕ_1 can be defined to point to the interior of $\mathcal{K}_i$, and also one has $u_1 \neq 0$. This implies that system trajectories do not escape the connectivity region. Setting $\beta = 0$ implies that $u_1 = \omega_1 = 0$, which means that system trajectories stay on $\partial\mathcal{K}_1$. This implies that the position trajectories $\boldsymbol{r}_1(t)$ starting in $\mathcal{K}_1$ never cross the boundary of $\mathcal{K}_1$, i.e., never escape the connectivity region O, and also that they are asymptotically stable to $\boldsymbol{r}_{1d}$, except for the set of initial conditions of measure zero corresponding to $\beta = 0$, i.e., except for initial positions on the boundary $\mathcal{K}_1$. This completes the proof on the connectivity maintenance and on the convergence to the goal destination for agent 1. ■

APPENDIX B
PROOF OF THEOREM 3

Proof: In order to design control strategies for the followers $j \neq 1$ one may employ the function V_j given by (17) as a candidate Lyapunov-like function for each agent j.

A. Non-overlapping sensing regions

Let us first consider the case when none of the remaining $N-1$ agents ever lies in the sensing region of agent j, i.e., that $d_{jk}(t) > R_s$, $\forall t \in [0,\infty)$, $\forall k \in \{1,\ldots,N\}$, $k \neq j$.

The Lyapunov-like function V_j is then taken out of (17) with $V_{jk} = 0$ $\forall k \in \{1,\ldots,N\}$, $k \neq j$, since one has $\sigma_{jk} = 0$ out of (14). No collisions occur, apparently, while the analysis on proximity maintenance and convergence to desired destination $\boldsymbol{r}_{jd}$ follows the same pattern as in Theorem 2.

B. Overlapping sensing regions

Let us now consider the worst-case when all the remaining $N-1$ agents initiate or happen to lie in the sensing area of agent j. The Lyapunov-like function (17) for agent j is:

$$V_j(\boldsymbol{r}_j, \boldsymbol{r}_{jd}, \boldsymbol{r}_k) = \frac{\left(\sum_{k\neq j} {V_{jk}}^{\delta}\right)^{\frac{1}{\delta}}}{1+\left(\sum_{k\neq j} {V_{jk}}^{\delta}\right)^{\frac{1}{\delta}}}, \tag{24}$$

where $k \in \{0, 1, \ldots, N\}$, $k \neq j$. The function V_j encodes proximity (or connectivity maintenance) for $k = 0$, collision avoidance w.r.t. the leader for $k = 1$, and collision avoidance w.r.t. the remaining followers for $k \neq j$. Its time derivative along the trajectories of agent j is:

$$\dot{V}_j = {\boldsymbol{\zeta}_j}^T \begin{bmatrix} \cos\theta_j \\ \sin\theta_j \end{bmatrix} u_j + \sum_{k=1, k\neq j}^{N} \left({\boldsymbol{\zeta}_{jk}}^T \begin{bmatrix} \cos\theta_k \\ \sin\theta_k \end{bmatrix} u_k \right), \tag{25}$$

where $\boldsymbol{\zeta}_j \triangleq \begin{bmatrix} \frac{\partial V_j}{\partial x_j} & \frac{\partial V_j}{\partial y_j} \end{bmatrix}^T$, $\boldsymbol{\zeta}_{jk} \triangleq \begin{bmatrix} \frac{\partial V_j}{\partial x_k} & \frac{\partial V_j}{\partial y_k} \end{bmatrix}^T$. Denote Γ_j the set where the gradients $\boldsymbol{\zeta}_j$, $\boldsymbol{\zeta}_{jk}$, and consequently the gradient ∇V_j, are not defined. More specifically, Γ_j is given as $\Gamma_j = \{\partial\mathcal{K}_j \bigcup \{\boldsymbol{r}_0\} \bigcup \{\boldsymbol{r}_k \mid \|\boldsymbol{r}_{jd} - \boldsymbol{r}_k\| = d_s\}\}$, where the boundary $\partial\mathcal{K}_j$ of the constrained set $\mathcal{K}_j$ comprises the boundary of the connectivity region and the boundary of the circular disk defining each agent $k \neq j$. Thus, defining the generalized gradient $\partial V_j(\cdot)$ at the points on the set $\partial\mathcal{K}_j \bigcup \{\boldsymbol{r}_0\}$ follows the same procedure as in Theorem A. Furthermore, at the points on the surface $S_{jk} = \{\boldsymbol{r}_k \mid \|\boldsymbol{r}_{jd} - \boldsymbol{r}_k\| = d_s\}$, one has that the generalized gradient is defined as the convex combination of the gradients on both sides of S_{jk}, which eventually reads: $\partial V_j(\cdot) = \nabla V_j$, since the gradient vectors on both sides of S_{jk} coincide and are equal to ∇V_j. In the sequel, with some abuse of notation, when referring to a gradient vector of the function V_j at a point p, we will be implying the standard gradient vector of V_j if $p \notin \Gamma_j$, and the Clarke generalized gradient vector if $p \in \Gamma_j$. As expected, the evolution of the time derivative $\dot{V}_j$ along the trajectories of agent j depends on the motion of the agents $k \neq j$ through their linear velocities u_k.

The proofs for the satisfaction of the desired objectives are given sequentially in the following three Lemmas. Briefly: first, we prove that the position trajectories and orientation trajectories of each agent j can be decomposed into slow and fast dynamics in a singular perturbations' sense. Second, we prove that the position trajectories of each agent are collision-free and remain in the connectivity region. Third, we prove that the position trajectories of each agent are almost globally convergent to its desired destination.

We first perform a time-scale decomposition of the agent's trajectories $\boldsymbol{q}_j(t)$ into fast and slow dynamics, in order to employ arguments related to singular perturbations [29]. We assume that the orientation trajectories $\theta_j(t)$ are controlled at a much faster time scale via the control law (19b) compared to the position trajectories $\boldsymbol{r}_j(t)$.[6] The system dynamics of agent j can then be decomposed into two subsystems, with the dynamics along the position trajectories $\boldsymbol{r}_j(t)$ serving as the reduced (slow) subsystem, and the orientation dynamics serving as the boundary-layer (fast) subsystem. Let us now consider the sufficiently small parameter $\varepsilon_j \triangleq \frac{1}{\lambda_j}$, and rewrite the closed-loop

[6]This is plausible for the unicycle-type vehicles that are considered here, such as for differentially-driven mobile robots.

boundary-layer (fast) dynamics as: $\frac{1}{\lambda_j}\,\dot{\theta}_j = -(\theta_j - \phi_j) + \frac{1}{\lambda_j}\,\dot{\phi}_j \Rightarrow \frac{1}{\lambda_j}\,\dot{\theta}_j = -(\theta_j - \phi_j) + \frac{1}{\lambda_j}\,\dot{\phi}_j \Rightarrow$

$$\varepsilon_j\,\dot{\theta}_j = -(\theta_j - \phi_j) + \varepsilon_j\dot{\phi}_j. \tag{26}$$

Lemma 2: The orientation θ_j of agent j is globally exponentially stable to ϕ_j.

Proof: The roots of the boundary-layer subsystem are given for $\varepsilon_j = 0$; out of (26) one has that the roots of the fast subsystem lie on the manifold $\theta_j = \phi_j$. Denote $\eta_j = \theta_j - \phi_j$ and take the dynamics:

$$\frac{d\eta_j}{dt} = \frac{d}{dt}(\theta_j - \phi_j) \overset{(26)}{=} -\frac{1}{\varepsilon_j}\,(\theta_j - \phi_j) = -\frac{1}{\varepsilon_j}\,\eta_j \Rightarrow$$
$$\varepsilon_j\,\frac{d\eta_j}{dt} = -\eta_j, \text{ which further reads: } \frac{d\eta_j}{d\tau} = -\eta_j,$$

where $\frac{d\tau}{dt} \triangleq \frac{1}{\varepsilon_j}$. The origin $\eta_j = 0$ of the boundary-layer subsystem is thus globally exponentially stable, which implies that θ_j is globally exponentially stable to ϕ_j. ■

Lemma 3: The control law (19) renders the constrained set $\mathcal{K}_j$ a positively invariant set for the reduced (slow) dynamics of agent j. This in turn implies that collision avoidance and proximity for agent j are guaranteed.

Proof: Avoiding collisions and maintaining proximity for agent j are encoded via ensuring that the constraint functions $c_{jk}(\boldsymbol{r}_j(t), \boldsymbol{r}_k(t)) \geq 0$, $\forall t, \forall (j,k)$. To prove this, we resort to set-theoretic analysis [23].

More specifically, the necessary and sufficient conditions for ensuring that the position trajectories $\boldsymbol{r}_j(t)$ starting in the set $\mathcal{K}_j$ always remain in $\mathcal{K}_j$ are given by Nagumo's theorem and read:

$$\frac{d}{dt}\,c_{jk}(\boldsymbol{r}_j, \boldsymbol{r}_k) \geq 0,\ \forall \boldsymbol{r}_j \in \partial\mathcal{K}_j,\ \forall (j,k).$$

This condition essentially states that the vector field of the system dynamics of agent j should always point into the interior of the constrained set $\mathcal{K}_j$.

1) Inter-agent Collision Avoidance: Let us consider the time derivative of the collision avoidance constraint

$$c_{jk} = (x_j - x_k)^2 + (y_j - y_k)^2 - {d_s}^2,\ k \in \{1, 2, \ldots, N\},$$

on the boundary of the constrained set $\mathcal{K}_j$, and evaluated at the equilibria $\theta_j = \phi_j$, $\theta_k = \phi_k$ of the boundary-layer (fast) subsystems of agents j, k, respectively, which reads:

$$\frac{d}{dt}\,c_{jk} = \underbrace{2u_j\,{\boldsymbol{r}_{kj}}^T \begin{bmatrix}\cos\phi_j \\ \sin\phi_j\end{bmatrix}}_{J}\ \underbrace{-2u_k\,{\boldsymbol{r}_{kj}}^T \begin{bmatrix}\cos\phi_k \\ \sin\phi_k\end{bmatrix}}_{K}, \tag{27}$$

where $\boldsymbol{r}_{kj} \triangleq \boldsymbol{r}_j - \boldsymbol{r}_k$ and the velocities u_j, u_k are positive by construction. Denote $\boldsymbol{\eta}_j \triangleq \begin{bmatrix}\cos\phi_j & \sin\phi_j\end{bmatrix}^T$, $\boldsymbol{\eta}_k \triangleq \begin{bmatrix}\cos\phi_k & \sin\phi_k\end{bmatrix}^T$ and let us provide the following definitions:

Definition 1: Assume that ${\boldsymbol{r}_{kj}}^T\boldsymbol{\eta}_j \geq 0$ and ${\boldsymbol{r}_{kj}}^T\boldsymbol{\eta}_k \leq 0$: Then $J \geq 0$ and $K \geq 0$, which implies that both agents j, k contribute in satisfying the collision avoidance condition. We say that collision avoidance is *"fully cooperative."*

Definition 2: Assume that ${\boldsymbol{r}_{kj}}^T\boldsymbol{\eta}_j \geq 0$ and ${\boldsymbol{r}_{kj}}^T\boldsymbol{\eta}_k \geq 0$: Then $J \geq 0$ and $K \leq 0$, which implies that agent j contributes towards avoiding collision, whereas agent k does not. If $J + K \geq 0$, we say that collision avoidance is *"semi-cooperative by agent j"*; otherwise, *"collision"* occurs.

Definition 3: Assume that ${\boldsymbol{r}_{kj}}^T\boldsymbol{\eta}_j \leq 0$ and ${\boldsymbol{r}_{kj}}^T\boldsymbol{\eta}_k \leq 0$: Then $J \leq 0$ and $K \geq 0$, which implies that agent k contributes towards avoiding collision, whereas agent j does not. If $J + K \geq 0$, we say that collision avoidance is *"semi-cooperative by agent k"*; otherwise, *"collision"* occurs.

Definition 4: Assume that ${\boldsymbol{r}_{kj}}^T\boldsymbol{\eta}_j \leq 0$ and ${\boldsymbol{r}_{kj}}^T\boldsymbol{\eta}_k \geq 0$: Then $J \leq 0$ and $K \leq 0$, which implies that *"collision"* occurs.

Recall our assumption that agent j may measure only the position vector $\boldsymbol{r}_k$ of agents k lying in its sensing region of radius R_s, i.e., can not measure the full state vectors $\boldsymbol{q}_k,\ \boldsymbol{\nu}_k$. In this respect, agent j may only determine the term J in (27), i.e., whether he/she contributes towards avoiding collision with agent k. Yet, this information is not enough to guarantee inter-agent collision avoidance, as illustrated in the definitions above. In addition, determining worst-case conditions on J and K is in general intractable, since: the vectors $\boldsymbol{\eta}_j$, $\boldsymbol{\eta}_k$ denote the directions of the negated gradient vector fields $-\boldsymbol{\zeta}_j$, $-\boldsymbol{\zeta}_k$ evaluated on the boundary of the constrained sets $\mathcal{K}_j$, $\mathcal{K}_k$, respectively, and thus they depend on the number and the relative positions of the agents in conflict. Furthermore, the linear velocities u_j, u_k are dependent on the current positions and goal destinations.

In view of these, we assume that each agent j does exchange information on linear velocities and orientations, yet only with agents lying within a circular safety region of radius R_c, where $d_s < R_c < R_z$, see Fig. 1. Within the safety region we define the following conflict resolution and coordination protocol:

Case 1: Agent j is in conflict with an agent $k \neq 1$.

- $J \geq 0$: Agent j moves away from or maintains fixed distance w.r.t., agent k. Collision avoidance may then be either "fully cooperative" or "semi-cooperative by agent j", depending on the effect of agent k in (27) via the term K. Collision occurs if and only if K is negative enough to render the condition (27) negative. We let agent j move with linear velocity:

$$u_{jc} = k_j \tanh(\|\boldsymbol{r}_j - \boldsymbol{r}_{jd}\|). \tag{28}$$

  The case of agent k moving so that $J + K < 0$ is excluded through the coordination imposed below.

- $J < 0$: Agent j moves towards agent k. Collision is avoided if and only if the term K renders the condition (27) positive, i.e., avoiding collision is, at best, "semi-cooperative by agent k." Nevertheless, agent j ignores the intentions of agent k. Thus, a way to ensure that $J + K \geq 0$ is to have agent j suitably adjust its linear velocity u_j. To this end we assume that, within the safety region, agent j communicates with agent k, acquires its linear velocity u_k and orientation ϕ_k, and moves according to:

$$u_{j|k} = u_{jc}\frac{d_{jk} - d_s}{R_c - d_s} + u_{js|k}\frac{R_c - d_{jk}}{R_c - d_s}, \tag{29}$$

  where:

$$u_{js|k} \leq u_k \frac{{\boldsymbol{r}_{kj}}^T\boldsymbol{\eta}_k}{{\boldsymbol{r}_{kj}}^T\boldsymbol{\eta}_j} \tag{30}$$

  is the safe (i.e., collision avoiding) velocity for agent j w.r.t. agent k dictated by the condition (27), and d_{jk} is the distance between j and k. A straightforward option is to set $u_{js|k}$ satisfying the equality in (30). The velocity profile $u_{j|k}$ in (29) is depicted in Fig. 5.

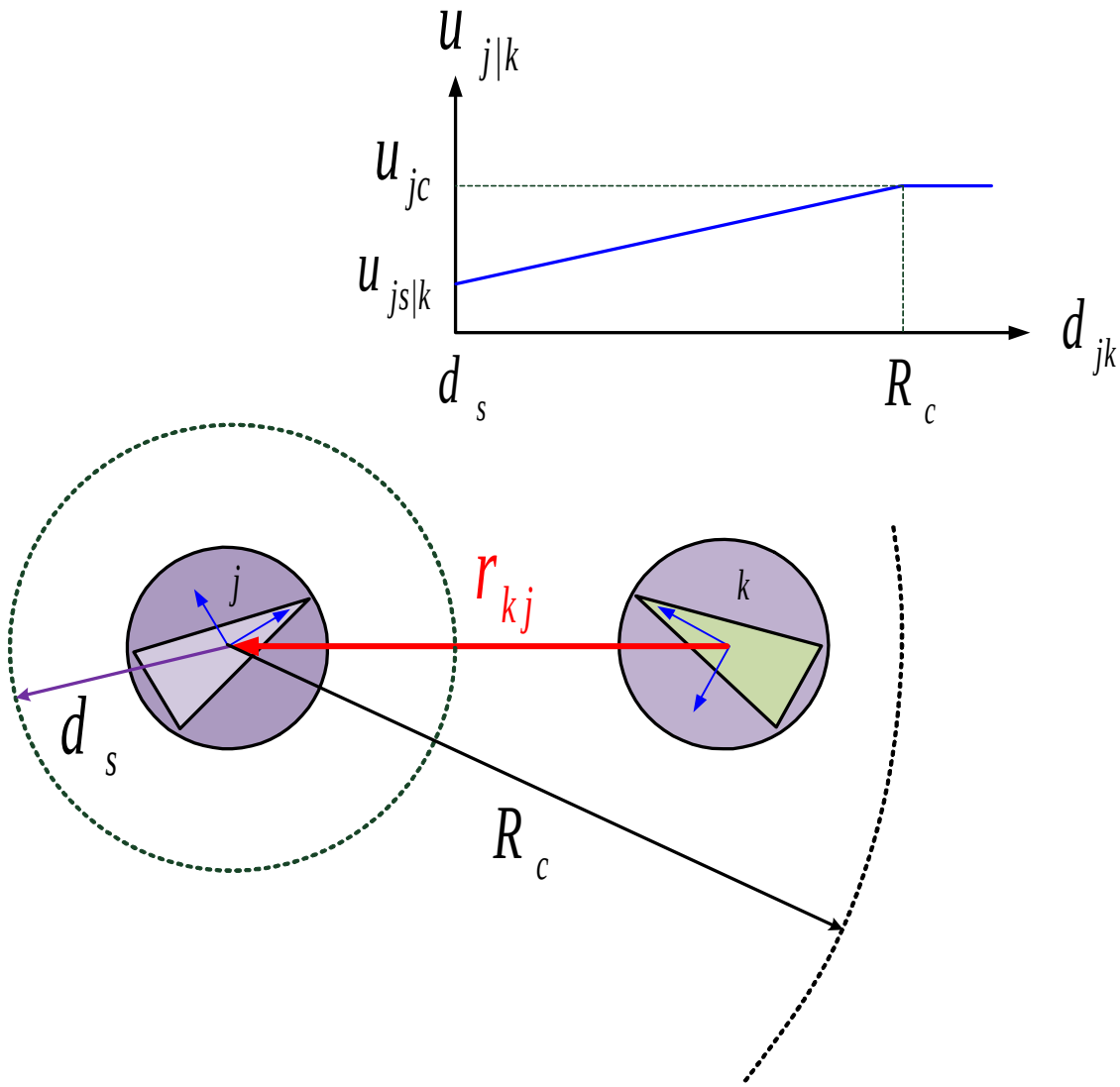

Fig. 5. If ${\boldsymbol{r}_{kj}}^T \boldsymbol{\eta}_j < 0$, i.e., if agent j moves towards agent k, then agent j adjusts its linear velocity according to the velocity profile shown here, given analytically by (29).

Under this choice, it is easy to verify that:

1) If ${\boldsymbol{r}_{kj}}^T \boldsymbol{\eta}_k > 0$, i.e., if agent k is moving towards agent j, then $u_{js|k} < 0$, which implies that the linear velocity u_j in (29) decreases. Depending also on the magnitude of $u_{jc} = k_j \tanh(\|\boldsymbol{r}_j - \boldsymbol{r}_{jd}\|)$, the linear velocity u_j may become negative. This verifies that if agent j lies on its goal destination $\boldsymbol{r}_{jd}$, then it will move away from its goal destination to facilitate collision avoidance with agent k.
2) If ${\boldsymbol{r}_{kj}}^T \boldsymbol{\eta}_k < 0$, i.e., if agent k is moving away from agent j, then $u_{js|k} > 0$. This implies that the linear velocity u_j in (29) may increase. Nevertheless, on the boundary of the constrained set $\mathcal{K}_j$, the velocity u_j is equal to the safe velocity $u_{js|k}$, implying that collision with agent k is avoided.

Denote the set of follower (homogenous) agents i that lie in the safety region of agent j with $\mathcal{I} = \{k, l, m, \dots\}$, and $J_i \triangleq \boldsymbol{r}_{ij}{}^T \boldsymbol{\eta}_j$. Then, a sufficient condition for agent j to avoid collisions is to adjust its linear velocity as:

$$u_j^\star = \min_{i \in \mathcal{I} | J_i < 0} u_{j|i}. \tag{31}$$

Case 2: Agent j is in conflict with the leader, $k = 1$. In this case, the leader ignores agent j by definition.

- $J \geq 0$: Agent j moves away from or maintains a constant distance w.r.t. the leader. The motion of the leader may though render the condition (27) negative. Worst-case, one has $K = -2u_1 \|\boldsymbol{r}_{1j}\| = -2u_1 d_s$. Then, agent j avoids the leader as long as: $u_{j|1} \geq \frac{u_1 d_s}{\boldsymbol{r}_{1j}{}^T \boldsymbol{\eta}_j}$. This yields the sufficient safe velocity:

  $$u_{js|1} = \frac{k_1 d_s}{\boldsymbol{r}_{1j}{}^T \boldsymbol{\eta}_j}, \text{ since } u_1 \leq k_1.$$

  Similarly to the case above, agent j needs to adjust its linear velocity in the proximity of the leader, when the leader lies a circular region of radius $d_1 < R_c$ around agent j, according to:

  $$u_{j|1} = u_{jc} \frac{d_{j1} - d_1}{d_1 - d_s} + u_{js|1} \frac{d_1 - d_{j1}}{d_1 - d_s}, \tag{32}$$

  see also Fig. 6.
- $J < 0$: Agent j moves towards the leader. For the worst-case effect of the leader through $K = -2u_1 d_s$, agent j needs to adjust its linear velocity according to (32). Note that here one has $u_{js|1} < 0$, which implies that the linear velocity u_j decreases.

Finally, recall that the leader is by definition uninvolved in avoiding collision with agent j, in the sense that it does not share information with any of the followers regarding to its state vector $\boldsymbol{q}_1$, $\boldsymbol{\nu}_1$. Thus it remains to agent j to ensure that the velocity $u_{j|1}$ dictating the avoidance of the (heterogenous) leader is consistent with the velocity $u_j^\star$, dictating the avoidance of the (homogenous) followers.

More specifically: If $u_j^\star$ dictates that agent j needs to slow down to avoid followers, and at the same time $u_{j|1}$ dictates that agent j needs to speed up to avoid the leader—in other words, if $u_j^\star < u_{j|1}$— then collision avoidance for agent j w.r.t. all agents is not guaranteed.

Therefore, as a last resort, agent j stops moving and communicates a signal to the leader, with which the leader realizes agent j as a static obstacle. Then, the leader updates its Lyapunov-like function V_1 by incorporating a squared recentered barrier function V_{1j} which encodes collision avoidance w.r.t. j, see also Remark 3. Collision avoidance between agent j and the leader is then accomplished by the leader. □

2) Proximity Maintenance: Let us now consider the time derivative of the proximity constraint $c_{j0} = R^2 - \|\boldsymbol{r}_j - \boldsymbol{r}_0\|$ on the boundary of the constrained set $\mathcal{K}_j$ and evaluated at the equilibrium $\theta_j = \phi_j$ of the boundary-layer (fast) subsystem of agent j, which after some algebraic calculations reads:

$$\frac{d}{dt} c_{j0} = -2u_j \frac{\boldsymbol{r}_{0j}{}^T \boldsymbol{\eta}_j}{\|\boldsymbol{r}_{0j}\|}, \tag{33}$$

where $\boldsymbol{r}_{0j} \triangleq \boldsymbol{r}_j - \boldsymbol{r}_0$. Now, consider the following cases:

1) Agent j is not in conflict with any other agent $k \neq 0$; then, it is straightforward to verify that $\boldsymbol{r}_{0j}{}^T \boldsymbol{\eta}_j \leq 0$, which implies that $\frac{d}{dt} c_{j0} \geq 0$, i.e., that the proximity constraint is not violated.

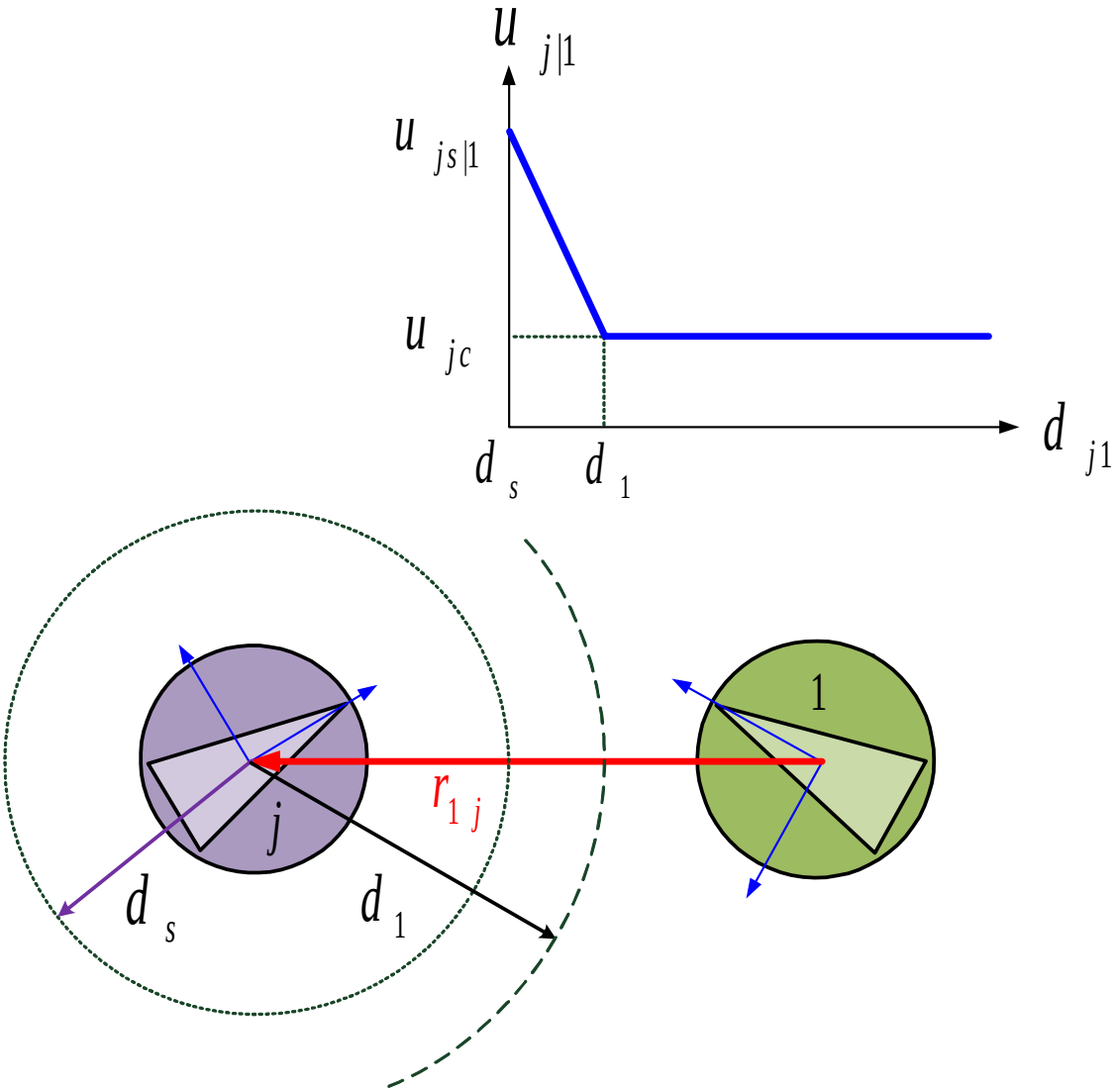

Fig. 6. To ensure avoidance of the leader, agent j needs to adjust its linear velocity according to (32) when the distance d_{j1} becomes less than a predefined distance d_1. If this adjustment is in conflict with avoiding possible followers in the safety region, then agent j stops and communicates a last resort signal to the leader, declaring himself as a static obstacle.

2) Agent j is at the same time in conflict with at least one agent $k \neq j$; then the signum of (33) depends on the number and relative position of the agents in conflict through the term $\boldsymbol{\eta}_j$. Worst-case, if ${\boldsymbol{r}_{0j}}^T \boldsymbol{\eta}_j > 0$, i.e if agent j is forced to violate the proximity constraint due to the effect of other conflicting agents, then agent j stops moving. □

Consequently, since $\frac{d}{dt}\, c_{jk}(\boldsymbol{r}_j, \boldsymbol{r}_k) \geq 0,\ \forall \boldsymbol{r}_j \in \partial\mathcal{K}_j,\ \forall j$, one has out of Nagumo's theorem [23] that the position trajectories $\boldsymbol{r}_j(t)$ starting in $\mathcal{K}_j$ never escape $\mathcal{K}_j$. This implies that under (19) the objectives of avoiding collisions and maintaining proximity for any agent $j \in \{2, \ldots, N\}$ w.r.t. any agent $k \in \{1, \ldots, N\}$, $j \neq k$, are always accomplished. Furthermore, (18) ensures that proximity is maintained for the leader. This completes the proof for

guaranteeing the collision avoidance and proximity objectives for the multi-agent system. ■

Lemma 4: Each agent j converges almost surely to its goal destination $\boldsymbol{r}_{jd}$.

Proof: For studying the convergence of agent j to the goal destination $\boldsymbol{r}_{jd}$, let us go back to the derivative of the Lyapunov-like function V_j for the reduced (slow) subsystem of agent j, evaluated at the equilibria $\theta_j = \phi_j$, $\theta_k = \phi_k$ of the boundary-layer subsystem:

$$\dot{V}_j = {\boldsymbol{\zeta}_j}^T \begin{bmatrix} \cos\phi_j \\ \sin\phi_j \end{bmatrix} u_j + \sum_{k=1,k\neq j}^{N} \left({\boldsymbol{\zeta}_{jk}}^T \begin{bmatrix} \cos\phi_k \\ \sin\phi_k \end{bmatrix} u_k \right). \tag{34}$$

The angles ϕ_j and ϕ_k are by definition the orientations of the vectors $-\boldsymbol{\zeta}_j$ and $-\boldsymbol{\zeta}_k$ respectively. Thus, one can write:

$$-\frac{\partial V_j}{\partial x_j} = \|\boldsymbol{\zeta}_j\| \cos\phi_j, \text{ and } -\frac{\partial V_j}{\partial y_j} = \|\boldsymbol{\zeta}_j\| \sin\phi_j,$$

where $\|\cdot\|$ stands for the standard Euclidean norm; this holds accordingly for subscript k. Substituting into (34) yields:

$$\dot{V}_j = -\|\boldsymbol{\zeta}_j\| u_j - \sum_{k=1,k\neq j}^{N} \left(\frac{{\boldsymbol{\zeta}_{jk}}^T \boldsymbol{\zeta}_k}{\|\boldsymbol{\zeta}_k\|} u_k \right). \tag{35}$$

Case 1: Assume that the safety regions of the agents never overlap, i.e., $R_c < d_{jk}(t) < R_s$, $\forall (j,k)$.

The control laws (18a), (19a) dictate that all N agents move with bounded positive linear velocities which vanish only at the corresponding desired destinations. The motion of agents $k \neq j$ can be seen as a perturbation to the position trajectories $\boldsymbol{r}_j(t)$ of agent j. The perturbation term involving the velocities u_k for $k \neq j$ depends on the agents' configurations $\boldsymbol{q}_k$ (through the vectors $\boldsymbol{\zeta}_{jk}$, $\boldsymbol{\zeta}_k$) and their destinations $\boldsymbol{r}_{kd}$ (through the control laws for u_k). Thus, $\dot{V}_j$ may be even increasing, depending on the signum of the second term including the effect of the other agents' velocities u_k. One way to deal with this is to use differential inequalities to establish a sufficient condition for accomplishing the objectives, as proposed in [30]. Yet, finding a comparison system for bounding the solutions of the considered system is not trivial. In order to bound the time derivative of V_j let us write:

$$\dot{V}_j \leq -\|\boldsymbol{\zeta}_j\| u_j + \sum_{k=1,k\neq j}^{N} \|\boldsymbol{\zeta}_{jk}\| u_k. \tag{36}$$

Then, one can take $\mu_1 \in (0,1)$ and $\mu_2 > 1$ so that: $\mu_1 V_j < \|\boldsymbol{\zeta}_j\|$, $\sum_{k=1,k\neq j}^{N} \|\boldsymbol{\zeta}_{jk}\| < \mu_2 V_j$, respectively.[7] Thus, (36) reads:

$$\dot{V}_j \leq -\mu_1 V_j k_j \tanh(\|\boldsymbol{r}_j - \boldsymbol{r}_{jd}\|) + \max_{k\neq j}\{u_k\} \mu_2 V_j.$$

Similarly, one may pick: $\nu_1 \in (0,1)$ so that: $\nu_1 \tanh(\|\boldsymbol{r}_j - \boldsymbol{r}_{jd}\|) < V_j$, to further write:

$$\dot{V}_j \leq -\mu_1 \nu_1 k_j \tanh^2(\|\boldsymbol{r}_j - \boldsymbol{r}_{jd}\|) + \max_{k\neq j}\{u_k\} \mu_2,$$

[7]Note that this is always possible, since the terms $\|\boldsymbol{\zeta}_j\|$, $\|\boldsymbol{\zeta}_{jk}\|$ are evaluated away from the boundary of the constrained set $\mathcal{K}_j$, and therefore are bounded.

which implies that V_j is an ISS local Lyapunov function for the position error $\boldsymbol{e}_j(t) \triangleq \boldsymbol{r}_j(t) - \boldsymbol{r}_{jd}$ on a compact subset of the constrained set $\mathcal{K}_j$. This further implies that, as t increases, $\boldsymbol{e}_j(t)$ is bounded by a class $\mathcal{K}$ function of $\sup_{t>t_0}(\max_{k\neq j}\{u_k(t)\})$. Furthermore, out of the ISS property, if $\max_{k\neq j}\{u_k(t)\}$ converges to zero as $t \to +\infty$, so does the error $\boldsymbol{e}_j(t)$, i.e., $\boldsymbol{r}_j(t) \to \boldsymbol{r}_{jd}$ [29].

To check whether the perturbation signal $\max_{k\neq j}\{u_k(t)\}$ converges to zero as $t \to +\infty$, note that $u_k(t)$ is a class $\mathcal{K}$ function of the position error $\boldsymbol{e}_k(t) = \boldsymbol{r}_k(t) - \boldsymbol{r}_{kd}$, see (19a). Nevertheless, the dynamics of $\boldsymbol{e}_k(t)$ are similarly governed by the signals $u_l(t)$ of the $l \neq k$ remaining agents. In other words, the ISS subsystems governing the evolution of the agents' position trajectories are feedback interconnected. This may tempt one to pursue sufficient conditions on the stability of the multi-agent system with analysis techniques such as small-gain theorems. In the case of complex systems, however, such techniques in principle require non-trivial, ad-hoc bounding of the derivatives, which may be intractable, or may lead to very conservative gain estimates.

Thus, let us note that the control law (19) essentially forces each agent j to perform gradient-descent along the level sets of V_j. It is expected that V_j has critical points other than the goal destination $\boldsymbol{r}_{jd}$, i.e., points $\bar{\boldsymbol{r}}_j$ at which the gradient vanishes, $\nabla V_j\big|_{\bar{\boldsymbol{r}}_j} = 0$. Clearly, the control law (19a) for u_j does not depend on ∇V_j, but instead vanishes at the goal destination $\boldsymbol{r}_{jd}$ only. Thus, the position trajectories $\boldsymbol{r}_j(t)$ can not identically stay on a critical point $\bar{\boldsymbol{r}}_j$, except for the singleton $\boldsymbol{r}_{jd}$. Nevertheless, the type of a critical point dictates the behavior of the negated gradient vector field (which here is used as reference through (19b)) in the vicinity of it. In particular, a local minimum is reached by all streamlines in its neighborhood, while a saddle point is reached by at most two streamlines in its neighborhood [31]. Then, tracking the gradient vector field via (19) in the vicinity of a possible local minimum $\bar{\boldsymbol{r}}_j \neq \boldsymbol{r}_{jd}$ will force the trajectories $\boldsymbol{r}_j(t)$ to perform infinite switching (chattering) around it. On the other hand, the set of initial conditions that approach a saddle point is of measure zero. In fact, it is known that the best one may achieve when resorting to gradients of scalar functions in constrained environments is to ensure that their critical points away from the desired destination are saddles, i.e., unstable equilibria; then, convergence to the goal is ensured almost everywhere, i.e., except for a set of initial conditions of measure zero.

In our case we have: $\nabla V_j = \frac{\nabla v_j}{(1+v_j)^2}$, which implies that the critical points of V_j are located at the critical points of v_j. The gradient of v_j is: $\nabla v_j = \frac{1}{\delta}\left(\sum (V_{jk})^\delta\right)^{\frac{1}{\delta}-1} \nabla\left(\sum (V_{jk})^\delta\right)$, and vanishes for $\sum (V_{jk})^\delta = 0$ or for $\nabla\left(\sum (V_{jk})^\delta\right) = 0$. The first condition yields that ∇v_j vanishes at the desired destination $\boldsymbol{r}_{jd}$. The second condition yields that the critical points of v_j are given as the solutions of: $\nabla\left(\sum (V_{jk})^\delta\right) = 0 \Rightarrow$

$$\delta\, {V_{j0}}^{\delta-1} \nabla V_{j0} + \sum_{\substack{k=0\\k\neq j}}^{N} \left(\delta\, (\sigma_{jk}\, {q_{jk}}^2)^{\delta-1}\, \nabla(\sigma_{jk}\, {q_{jk}}^2)\right) = 0. \tag{37}$$

Clearly, the location of the critical points of v_j is reactive, in the sense that it depends on the current positions of the agents and on the goal destinations. To demonstrate this, consider the simplest case when only one agent $k \neq 0$ lies in the sensing region of agent j, so that the inter-agent distance is $d_{jk} < R_z$, which yields $\sigma_{jk} = 1$. The critical manifold reduces into ${r_{j0}}^{2\delta-1}\nabla r_{j0} + {q_{jk}}^{2\delta-1}\nabla q_{jk} = 0$. The solutions of this equation are either the goal position $\boldsymbol{r}_{id}$, or a critical point $\bar{\boldsymbol{r}}_j$ which appears in the case when the gradient vectors ∇r_{j0}, ∇q_{jk} oppose to each

other. This further reads that $\bar{\boldsymbol{r}}_j$ lies on the line which connects the current position $\boldsymbol{r}_k$ of agent k with the goal destination $\boldsymbol{r}_{jd}$ of agent j, at some distance w.r.t. the point $\boldsymbol{r}_k$ which depends on δ, r_{j0}, q_{jk}.

In order to ensure that a critical point $\bar{\boldsymbol{r}}_j$ of V_j is saddle (unstable equilibrium), one may resort to the Hessian matrix test; if the Hessian matrix $\nabla^2 V_j$ evaluated at the critical point $\bar{\boldsymbol{r}}_j$, has both negative and positive eigenvalues, then $\bar{\boldsymbol{r}}_j$ is a saddle point. Tuning the parameter δ that appears in $\nabla^2 V_j$ is non-trivial since the Hessian depends on the system parameters δ, d_s, $\boldsymbol{r}_{jd}$ and on the (dynamic) positions $\boldsymbol{r}_k$, $\boldsymbol{r}_j$.[8] In this respect, we argue that:

Proposition 1: The probability for agent j to get stuck to a critical point other than its goal destination is zero.

Proof: To justify this, let us first consider that only one agent k lies in the sensing region of agent j: Then, the agents get stuck away from their goal destinations only if they both lie on the undesired critical point of their corresponding Lyapunov-like functions V_j, V_k, which implies that their positions and goal destinations lie on the same line. Let us now assume that two agents k, l lie in the sensing region of agent j. The agents k, l can not be both at their goal destinations, since this would imply that $\|\boldsymbol{r}_{kd} - \boldsymbol{r}_{ld}\| < 2\, R_s$, i.e., a contradiction. Assume that all agents lie away from their goal destinations. Then agents get stuck only if all of them lie on a critical point of their corresponding Lyapunov-like functions; if at least one of them does not lie on a critical point, then its motion will affect the position of the other agents' critical points, forcing them to escape. Assume now that agents j and k lie away from their goal destinations, while agent l lies on this goal destination. Then again, agents j and k get stuck only if they both lie on a critical point of their corresponding V_j, V_k. In this case, agent l does not facilitate with its motion the other two agents to escape their critical points, yet the case reduces into the $N = 2$ agent case described above, with the agents getting stuck only if their positions and goal destinations satisfy the solution of (37). The same reasoning can be adopted for the $N > 3$ case. ■

This completes the proof for the almost sure convergence to the desired destinations for the multi-agent system, for the case that only the sensing (not the safety) regions of the agents overlap during the system evolution.

Case 2: Assume that the safety regions of the agents overlap, i.e., $d_s < d_{jk}(t) < R_c$, $\forall (j,k)$. Then the control laws (19a) of the followers dictate that an agent may need to stop at a point away from its desired destination, to avoid a worst-case collision w.r.t. the leader. In any other case, the analysis on getting stuck at undesired locations follows the same pattern as before.

This completes the proof for the almost sure convergence to the desired destinations for the multi-agent system, for the case that the safety regions of the agents overlap during the system evolution. ■

The analysis on the cases of overlapping sensing regions and overlapping safety regions dictate that agent j almost surely converges to its desired destination.

In summary, the results in Lemmas 1, 2 and 3 guarantee the accomplishment of the desired objectives (collision avoidance and connectivity maintenance), under the caveat that convergence to desired destinations is almost sure. ■

[8] In general, obtaining sufficient lower bounds for δ as analytic functions depends on the characteristics of the problem at hand. It is worth mentioning that the parameter δ of the Lyapunov-like function V_j essentially works in an analogous way as the tuning parameter κ of a navigation function in the Rimon-Koditschek sense [32], which implies that all undesired local minima of V_j disappear as κ increases.

APPENDIX C
PROOF OF THEOREM 4

Proof: We first consider the convergence of the leader agent $k = 1$ w.r.t. the moving destination $\boldsymbol{r}_{1d}$, and then the avoidance of the connectivity boundary.

Convergence: To analyze the behavior of the position trajectories of the leader let us take the time derivative of the Lyapunov function V_1 of the nominal system, evaluated at the root $\theta_1 = \phi_1$ of the boundary-layer subsystem, which reads:

$$\dot{V}_1 = {\boldsymbol{\zeta}_1}^T \begin{bmatrix} \cos\phi_1 \\ \sin\phi_1 \end{bmatrix} u_1 - {\boldsymbol{\zeta}_1}^T \dot{\boldsymbol{r}}_{1d} + {\boldsymbol{\zeta}_{10}}^T \dot{\boldsymbol{r}}_0 = -k_1 \|\boldsymbol{\zeta}_1\|$$
$$- {\boldsymbol{\zeta}_1}^T \dot{\boldsymbol{r}}_{1d} + {\boldsymbol{\zeta}_{10}}^T \dot{\boldsymbol{r}}_0 \leq -(k_1 - k_d)\|\boldsymbol{\zeta}_1\| + k_d \|\boldsymbol{\zeta}_{10}\|,$$

where $\boldsymbol{\zeta}_1 \triangleq \begin{bmatrix} \frac{\partial V_1}{\partial x_1} & \frac{\partial V_1}{\partial y_1} \end{bmatrix}$, $\boldsymbol{\zeta}_{10} \triangleq \begin{bmatrix} \frac{\partial V_1}{\partial x_0} & \frac{\partial V_1}{\partial y_0} \end{bmatrix}$ and $\|\boldsymbol{\zeta}_1\|$, $\|\boldsymbol{\zeta}_{10}\|$ are class $\mathcal{K}_\infty$ functions. Furthermore, away from the boundary $\partial\mathcal{K}_{10}$, i.e., away from the boundary of the connectivity region one has that $\|\boldsymbol{\zeta}_{10}\| \leq \|\boldsymbol{\zeta}_1\|$. Then:

$$\dot{V}_1 \leq -(k_1 - 2k_d)\|\boldsymbol{\zeta}_1\|.$$

If the connectivity region O is free of static obstacles, then the gradient vector $\boldsymbol{\zeta}_1$ vanishes at the goal destination $\boldsymbol{r}_{1d}$ only. Thus, for $k_1 > 2k_d$, the derivative of V_1 is negative and vanishes at the goal destination $\boldsymbol{r}_{1d}$ only, i.e., the position trajectories $\boldsymbol{r}_1(t)$ of the leader agent are locally asymptotically stable w.r.t. the dynamic (moving) goal destination $\boldsymbol{r}_{1d}$ in a compact subset of the constrained set $\mathcal{K}_{10}$.

Maintaining connectivity: Let us now take the time derivative of the proximity constraint $c_{10} = R - \|\boldsymbol{r}_1 - \boldsymbol{r}_0\|$ on the boundary of the constrained set $\mathcal{K}_1$ and evaluated at the equilibrium $\theta_1 = \phi_1$ of the boundary-layer (fast) subsystem of agent 1, which reads:

$$\frac{d}{dt}\, c_{10} = -\frac{2k_1}{\|\boldsymbol{r}_{01}\|} {\boldsymbol{r}_{01}}^T \begin{bmatrix} \cos\phi_1 \\ \sin\phi_1 \end{bmatrix} + \frac{2}{\|\boldsymbol{r}_{01}\|} {\boldsymbol{r}_{01}}^T \begin{bmatrix} \dot{x}_0 \\ \dot{y}_0 \end{bmatrix}, \tag{38}$$

where $\boldsymbol{r}_{01} \triangleq \boldsymbol{r}_1 - \boldsymbol{r}_0$. It is easy to verify that ${\boldsymbol{r}_{01}}^T \left[\begin{smallmatrix} \cos\phi_1 \\ \sin\phi_1 \end{smallmatrix}\right] = -\|\boldsymbol{r}_{01}\|$, which implies that the first term is always positive. Let us consider that the effect of the second term is as negative as possible, i.e., that ${\boldsymbol{r}_{01}}^T \left[\begin{smallmatrix} \dot{x}_0 \\ \dot{y}_0 \end{smallmatrix}\right] = -\|\boldsymbol{r}_{01}\| k_d$. Then, the derivative of the constraint function (38) reads:

$$\frac{d}{dt}\, c_{10} = 2k_1 - 2k_d = 2(k_1 - k_d),$$

which is positive since $k_1 > 2k_d$, implying that the position trajectories $\boldsymbol{r}_1(t)$ remain always in the connectivity region O. ■

APPENDIX D
PROOF OF THEOREM 5

Proof: Similarly to the analysis in Theorem 4, we consider the evolution of the perturbed trajectories for each agent j w.r.t. the nominal Lyapunov-like function V_j.

Convergence to a ball around the goal destination: Let us consider the worst case when all agents lie in the sensing region of agent j. To analyze the behavior of the position trajectories $\boldsymbol{r}_j(t)$ agent j let us take the time derivative of the Lyapunov-like function V_j of the nominal system, evaluated at the roots of the boundary-layer subsystem:

$$\begin{aligned}\dot{V}_j &= \boldsymbol{\zeta}_j^T \begin{bmatrix}\cos\phi_j\\ \sin\phi_j\end{bmatrix} u_j - \boldsymbol{\zeta}_j^T\, \dot{\boldsymbol{r}}_{jd} + \boldsymbol{\zeta}_{j0}^T\, \dot{\boldsymbol{r}}_0 + \sum_{\substack{k=1\\k\neq j}}^{N} \left(\boldsymbol{\zeta}_{jk}^T \begin{bmatrix}\cos\phi_k\\ \sin\phi_k\end{bmatrix} u_k\right)\\ &= -\|\boldsymbol{\zeta}_j\| u_j - \boldsymbol{\zeta}_j^T\, \dot{\boldsymbol{r}}_{jd} + \boldsymbol{\zeta}_{j0}^T\, \dot{\boldsymbol{r}}_0 + \sum_{\substack{k=1\\k\neq j}}^{N} \left(\boldsymbol{\zeta}_{jk}^T \begin{bmatrix}\cos\phi_k\\ \sin\phi_k\end{bmatrix} u_k\right)\\ &\leq -\|\boldsymbol{\zeta}_j\| u_j + k_d\|\boldsymbol{\zeta}_j\| + k_d\|\boldsymbol{\zeta}_{j0}\| + \sum_{k=1,k\neq j}^{N} \|\boldsymbol{\zeta}_{jk}\| u_k\end{aligned}$$

Then, similarly to the reasoning in Appendix B, one can take $\mu_1 \in (0,1)$ and $\mu_2, \mu_3, \mu_4 > 1$ such that: $\mu_1 V_j < \|\boldsymbol{\zeta}_j\|$, $\sum_{k=1,k\neq j}^{N} \|\boldsymbol{\zeta}_{jk}\| < \mu_2 V_j$, $k_d\|\boldsymbol{\zeta}_j\| < \mu_3 V_j$ and $k_d\|\boldsymbol{\zeta}_{j0}\| < \mu_4 V_j$. Thus, $\dot{V}_j$ reads:

$$\begin{aligned}\dot{V}_j &\leq -\mu_1 k_j V_j \tanh(\|\boldsymbol{r}_j - \boldsymbol{r}_{jd}\|) + (\max_{k\neq j}\{u_k\}\mu_2 + \mu_3 + \mu_4) V_j\\ &\leq -\mu_1 k_j \underbrace{V_j \tanh(\|\boldsymbol{r}_j - \boldsymbol{r}_{jd}\|)}_{\gamma_j(\cdot)} + \underbrace{\max\left\{\max_{k\neq j}\{u_k\}\mu_2, \mu_3, \mu_4\right\}}_{\delta_j(\cdot)},\end{aligned}$$

where the function $\gamma_j(\cdot) = V_j \tanh(\|\boldsymbol{r}_j - \boldsymbol{r}_{jd}\|)$ is a class $\mathcal{K}$ function of the position error $\boldsymbol{e}_j \triangleq \boldsymbol{r}_j - \boldsymbol{r}_{jd}$. Then, V_j is an ISS local Lyapunov function for the position error $\boldsymbol{e}_j(t)$ on a compact subset of the constrained set $\mathcal{K}_j$. This implies that, as t increases, $\boldsymbol{e}_j(t)$ is bounded by a class $\mathcal{K}$ function of $\sup_{t>t_0} \delta_j(\cdot) = \max\{k_k\mu_2, \mu_3, \mu_4\}$. Furthermore, the ISS property dictates that the position error trajectories $\boldsymbol{e}_j(t)$ approach the ultimate bound of the system, which depends on $\delta_j(\cdot)$. In other words, the position trajectories $\boldsymbol{r}_j(t)$ approach a ball around the goal destination $\boldsymbol{r}_{jd}(t)$ whose radius is dictated by the evolution of $\max\{\max_{k\neq j}\{u_k(t)\}\mu_2, \mu_3, \mu_4\}$. This term is, as expected, depended on the linear velocity k_d of the dynamic (moving) goal destination through the choice of μ_3, μ_4.

Maintaining connectivity: Let us now take the time derivative of the proximity constraint $c_{j0} = R - \|\boldsymbol{r}_j - \boldsymbol{r}_0\|$ on the boundary of the constrained set $\mathcal{K}_j$ and evaluated at the equilibrium $\theta_j = \phi_j$ of the boundary-layer (fast) subsystem of agent j, which reads:

$$\frac{d}{dt}\, c_{j0} = -\frac{2u_j}{\|\boldsymbol{r}_{0j}\|}{\boldsymbol{r}_{0j}}^T \begin{bmatrix}\cos\phi_j\\ \sin\phi_j\end{bmatrix} + \frac{2}{\|\boldsymbol{r}_{0j}\|}{\boldsymbol{r}_{0j}}^T \begin{bmatrix}\dot{x}_0\\ \dot{y}_0\end{bmatrix}, \tag{39}$$

where $\boldsymbol{r}_{0j} \triangleq \boldsymbol{r}_j - \boldsymbol{r}_0$. If only the proximity constraint is active, i.e., if agent j is not in conflict with any other agent, then it is easy to verify that ${\boldsymbol{r}_{0j}}^T \left[\begin{smallmatrix}\cos\phi_j\\ \sin\phi_j\end{smallmatrix}\right] = -\|\boldsymbol{r}_{0j}\|$, which implies that the first term is always positive. Worst case, the effect of the second term is as negative as possible, i.e., ${\boldsymbol{r}_{0j}}^T \left[\begin{smallmatrix}\dot{x}_0\\ \dot{y}_0\end{smallmatrix}\right] = -\|\boldsymbol{r}_{0j}\| k_d$. Then, the derivative (39) reads:

$$\frac{d}{dt}\, c_{j0} = 2u_j - 2k_d = 2(u_j - k_d),$$

which is positive for $u_j > k_d$. To ensure that this condition always holds one may: (i) set the goal destination $\boldsymbol{r}_{jd}$ sufficiently away from the connectivity boundary, i.e., in a circular region of radius $r_g = R_0 - r_a - R_s$ around the center $\boldsymbol{r}_0$ of the connectivity region; in this way: $u_j \geq k_j \tanh(R_s)$ (ii) set the velocity $k_d < k_j \tanh(R_s)$. Then, the proximity constraint is never violated, which implies that the position trajectories $\boldsymbol{r}_j(t)$ remain always in the connectivity region O. ■

REFERENCES

[1] W. Ren and Y. Cao, "Overview of recent research in distributed multi-agent coordination," in *Distributed Coordination of Multi-agent Networks*, ser. Communications and Control Engineering. Springer-Verlag London Limited, 2011, ch. 2, pp. 23–41.

[2] L. E. Parker, "Path planning and motion coordination in multiple mobile robot teams," in *Encyclopedia of Complexity and System Science*, R. A. Meyers, Ed. Springer, 2009.

[3] A. Jadbabaie, J. Lin, and A. S. Morse, "Coordination of groups of mobile autonomous agents using nearest neighbor rules," *IEEE Transactions on Automatic Control*, vol. 48, no. 6, pp. 988–1001, Jun. 2003.

[4] H. G. Tanner, "Flocking with obstacle avoidance in switching networks of interconnected vehicles," in *Proc. of the 2004 IEEE International Conference on Robotics and Automation*, New Orleans, LA, Apr. 2004, pp. 3006–3011.

[5] R. Olfati-Saber, "Flocking for multi-agent dynamic systems: Algorithms and theory," *IEEE Transactions on Automatic Control*, vol. 51, no. 3, pp. 401–420, Mar. 2006.

[6] H. G. Tanner, A. Jadbabaie, and G. J. Pappas, "Flocking in fixed and switching networks," *IEEE Transactions on Automatic Control*, vol. 52, no. 5, pp. 863–868, May 2007.

[7] B. Sharma, J. Vanualailai, and U. Chand, "Flocking of multi-agents in constrained environments," *European Journal of Pure and Applied Mathematics*, vol. 2, no. 3, pp. 401–425, 2009.

[8] H. Su, X. Wang, and Z. Lin, "Flocking of multi-agents with a virtual leader," *IEEE Transactions on Automatic Control*, vol. 54, no. 2, pp. 293–307, Feb. 2009.

[9] M. Ji and M. Egerstedt, "Distributed coordination control of multiagent systems while preserving connectedness," *IEEE Transactions on Robotics*, vol. 23, no. 4, pp. 693–703, Aug. 2007.

[10] R. Olfati-Saber, J. A. Fax, and R. M. Murray, "Consensus and cooperation in networked multi-agent systems," *Proceedings of the IEEE*, vol. 95, no. 1, pp. 215–233, Jan. 2007.

[11] D. V. Dimarogonas and K. J. Kyriakopoulos, "A connection between formation infeasibility and velocity alignment in kinematic multi-agent systems," *Automatica*, vol. 44, no. 10, pp. 2648–2654, Oct. 2008.

[12] S. Mastellone, D. M. Stipanović, C. R. Graunke, K. A. Intlekofer, and M. W. Spong, "Formation control and collision avoidance for multi-agent non-holonomic systems: Theory and experiments," *The International Journal of Robotics Research*, vol. 27, no. 1, pp. 107–126, Jan. 2008.

[13] D. V. Dimarogonas and K. J. Kyriakopoulos, "Connectedness preserving distributed swarm aggregation for multiple kinematic robots," *IEEE Transactions on Robotics*, vol. 24, no. 5, pp. 1213–1223, Oct. 2008.

[14] M. M. Zavlanos, M. B. Egerstedt, and G. J. Pappas, "Graph-theoretic connectivity control of mobile robot networks," *Proceedings of the IEEE*, vol. 99, no. 9, pp. 1525–1540, Sep. 2011.

[15] E. G. Hernandez-Martinez and E. Aranda-Bricaire, "Convergence and collision avoidance in formation control: A survey of the artificial potential functions approach," in *Multi-Agent Systems - Modeling, Control, Programming, Simulations and Applications*, ser. Robotics. Multiagent Systems, F. Alkhateeb, E. A. Maghayreh, and I. A. Doush, Eds. InTech, 2011, ch. 6, pp. 103–126.

[16] J. Cortes, S. Martínez, T. Karatas, and F. Bullo, "Coverage control for mobile sensing networks," *IEEE Transactions on Robotics and Automation*, vol. 20, no. 2, pp. 243–255, 2004.

[17] I. I. Hussein and D. M. Stipanović, "Effective coverage control for mobile sensor networks with guaranteed collision avoidance," *IEEE Transactions on Control Systems Technology*, vol. 15, no. 4, pp. 642–657, Jul. 2007.

[18] S. Berman, A. Halász, M. A. Hsieh, and V. Kumar, "Optimized stochastic policies for task allocation in swarms of robots," *IEEE Transactions on Robotics*, vol. 25, no. 4, pp. 927–937, Aug. 2009.

[19] M. Schwager, J.-J. Slotine, and D. Rus, "Unifying geometric, probabilistic, and potential field approaches to multi-robot coverage control," in *Tracts in Advanced Robotics*, ser. Robotics Research. Springer, 2011, vol. 70, pp. 21–38.

[20] A. Renzaglia, L. Doitsidis, A. Martinelli, and E. B. Kosmatopoulos, "Multi-robot three-dimensional coverage of unknown areas," *The International Journal of Robotics Research*, vol. 31, no. 6, pp. 738–752, 2012.

[21] F. Pasqualetti, A. Franchi, and F. Bullo, "On cooperative patrolling: Optimal trajectories, complexity analysis and approximation algorithms," *IEEE Transactions on Robotics*, vol. 28, no. 3, pp. 592–606, 2012.

[22] D. Panagou and V. Kumar, "Cooperative visibility maintenance for leader-follower formations in obstacle environments," *IEEE Transactions on Robotics*, vol. 30, no. 4, pp. 831–844, Aug. 2014.

[23] F. Blanchini and S. Miani, *Set-Theoretic Methods in Control*. Birkhauser, 2008.

[24] A. G. Wills and W. P. Heath, "A recentred barrier for constrained receding horizon control," in *Proc. of the American Control Conference*, Anchorage, AK, USA, May 2002, pp. 4177–4182.

[25] D. M. Stipanović, C. J. Tomlin, and G. Leitmann, "Monotone approximations of minimum and maximum functions and multi-objective problems," *Applied Mathematics and Optimization*, vol. 66, pp. 455–473, 2012.

[26] D. Panagou, D. M. Stipanović, and P. G. Voulgaris, "Multi-objective control for multi-agent systems using Lyapunov-like barrier functions," in *Proc. of the 52nd IEEE Conference on Decision and Control*, Florence, Italy, Dec. 2013, pp. 1478–1483.

[27] Y. Nesterov and A. Nemirovskii, *Interior Point Polynomial Algorithms in Convex Programming*. SIAM Studies in Applied Mathematics, 2001.

[28] M. Saska, J. S. Mejia, D. M. Stipanovic, and K. Schilling, "Control and navigation of formations of car-like robots on a receding horizon," in *Proc. of the 2009 IEEE Conference on Control Applications (CCA) and Intelligent Control (ISIC)*, Saint Petersburg, Jul. 2009, pp. 1761–1766.

[29] H. K. Khalil, *Nonlinear Systems. Third Edition*. Prentice-Hall Inc., 2002.

[30] D. M. Stipanović, C. Valicka, C. J. Tomlin, and T. R. Bewley, "Safe and reliable coverage control," *Numerical Algebra, Control and Optimization*, vol. 3, pp. 31–48, 2013.

[31] M. Henle, *A Combinatorial Introduction to Topology*. Dover Publications, 1994.

[32] E. Rimon and D. Koditschek, "Exact robot navigation using artificial potential functions," *IEEE Transactions on Robotics and Automation*, vol. 8, no. 5, pp. 501–518, Oct. 1992.